Article

Innovative Dual Combination Cospray-Dried Rock Inhibitor/L-Carnitine Inhalable Dry Powder Aerosols

Maria F. Acosta, David Encinas-Basurto, Michael D. Abrahamson, Basanth Babu Eedara, Don Hayes, Jr., Jeffrey R. Fineman, Stephen M. Black, and Heidi M. Mansour*

Read Online

ACCESS | 📊 Metrics & More | 📰 Article Recommendations

ABSTRACT: This study introduces novel cospray-dried (Co-SD) formulations of simvastatin, a Nrf2 activator ROCK inhibitor, with L-carnitine as molecular mixtures in various molar ratios for targeted pulmonary inhalation aerosol delivery in pulmonary hypertension, optimized for excipient-free dry powder inhalers (DPIs). The two components were spray-dried at various molar ratios by using different starting feed solution concentrations and process parameters. In addition to comprehensive physicochemical characterization, in vitro aerosol dispersion performance as DPIs using two FDA-approved DPI devices with different shear stress properties, in vitro viability as a function of dose on 2D human pulmonary cellular monolayers and on 3D small airway epithelia human primary cultures at the air−liquid interface (ALI), and in vitro transepithelial electrical resistance (TEER) at the ALI were conducted. Solid-state physicochemical characterization confirmed homogeneous molecular mixtures and the crystalline nature of the Co-SD formulations. In vitro aerosolization dispersion performance demonstrated that all Co-SD dual combination molecular mixtures aerosolized successfully with both human FDA-approved DPI devices, had ∼100% emitted dose, and good fine particle fraction values. The in vitro viability and TEER assays demonstrated that all formulations were safe to the human pulmonary cell as 2D and 3D cultures as a function of dose.

KEYWORDS: targeted pulmonary delivery, dry powder inhalers (DPIs), viability, Nrf2 activator ROCK inhibitor, transepithelial electrical resistance (TEER), pulmonary hypertension (PH), mitochondria
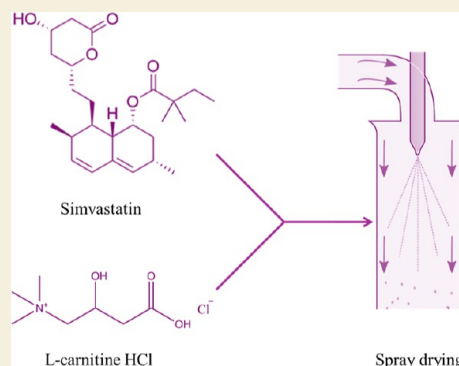
■ INTRODUCTION

Pulmonary drug delivery has become one of the most important routes for effectively targeting drugs to treat many respiratory diseases and for noninvasive systemic delivery.[1−4] Dry powder inhalers (DPIs) offer greater chemical stability of drugs, high dose delivery, minimal patient hand-lung coordination, absence of propellant, shorter inhalation treatment times, and the potential to tailor particle properties in the solid state in comparison with other aerosol delivery systems.[5,6]

Spray drying (SD) is a high-throughput process with the ability to engineer and produce particles in a more controlled manner (such as directing particle size and size distribution, particle, and surface morphology), which are important particle features particle features[7,8] for pulmonary dry powder drug delivery by inhalation. In addition, SD is an ideal technique for the microencapsulation of various types of drugs, both small molecules and large molecules.[9]

Pulmonary hypertension (PH) is complex and involves both the pulmonary and cardiovascular systems.[10] PH is a fatal disease that is characterized by increased pulmonary arterial pressure, endothelial inflammation due to the production of reactive oxygen species, and mitochondrial lung dysfunc-

tion.[11−14] Simvastatin (Sim) has potent antiproliferative and pro-apoptotic effects on vasculature smooth muscle cells through the inhibition of the synthesis of isoprenoid intermediates (geranylgeranyl pyrophosphate and farnesyl pyrophosphate), which are essential for the post-translational isoprenylation of Rho, Rac, and Ras family GTPases (intracellular signaling molecules whose proper membrane localization and function are dependent on the lipid character that isoprenoids offer to them).[15,16] Sim is a known Nrf2 activator and RhoA/Rho Kinase (ROCK) inhibitor that has been demonstrated to be effective in PH.[15]

Sim is known to have significant anti-inflammatory and antioxidant properties.[16] These effects are particularly important in the context of pulmonary diseases such as chronic obstructive pulmonary disease (COPD), asthma, and PH, where chronic

inflammation and oxidative stress play central roles in disease progression. Sim's ability to modulate inflammatory pathways and reduce oxidative damage makes it a promising candidate for inhalable therapies targeting the lungs.[17] L-Carnitine (L-Car) [(4-*N*-trimethylammonium-3-hydroxybutyric acid)] has been demonstrated to be effective in PH.[18,19] Our group was the first to demonstrate the effectiveness of these as individual DPIs in PH.[15,19]

Organic solution closed-mode advanced SD was employed to exploit the unique advantages of organic solvents (i.e., alcohols) over aqueous formulations in designing dry particles that are both inhalable and high performing as DPIs, as we have reported.[9,20−24] Uniform drug composition of two active pharmaceutical ingredients (APIs) can be accomplished by cospray drying a solution with the two active APIs, as we have recently reported as dual-drug carrier-free DPIs.[25] Synergistic effects in the damaged lung regions can be achieved due to the simultaneous deposition and colocalization in the same lung region (compared to delivering two separate individual aerosols in PH patients),[21] as has been demonstrated clinically to be superior in the treatment and management of asthma, cystic fibrosis, and COPD.[21]

This comprehensive and systematic study builds on our recent studies on advanced Sim DPIs[15] and L-Car DPIs,[19] as one-component advanced spray-dried inhalation powders for use in PH. To the authors' knowledge, this is the first report on dual-drug molecular mixture combination of a Nrf2 activator ROCK inhibitor with L-Car salt as cospray-dried (Co-SD) carrier-free inhalation aerosols as DPIs for targeted pulmonary delivery in PH.

MATERIALS AND METHODS

Materials

Sim [United States Pharmacopeia (USP) grade] [$C_{25}H_{38}O_5$; molecular weight (MW): 418.566 g/mol] was obtained from ACROS (New Jersey, New Jersey), and L-Car HCl salt, 98+% purity ($C_7H_{16}ClNO_3$; MW: 197.66 g/mol) was obtained from Sigma-Aldrich, Inc. (St. Louis, Missouri). Figure 1 shows the chemical structures (ChemDraw Ultra Ver. 15.0.; CambridgeSoft, Cambridge, Massachusetts) for Sim and L-Car. Methanol (HPLC grade, ACS-certified grade, purity 99.9%) was obtained from Fisher Scientific (Fair Lawn, New Jersey). Hydranal-Coulomat AD and resazurin sodium salt were obtained from Sigma-Aldrich, Inc. (St. Louis, Missouri). Raw Sim and L-Car HCl were stored in sealed glass desiccators over Indicating Drierite/Drierite desiccant at −20 °C under an ambient pressure. Other chemicals were stored under room conditions. The nitrogen was ultrahigh purity (UHP) gas was used (Cryogenics Gas Facility, The University of Arizona, Tucson, Arizona).

Human pulmonary cell lines A549 alveolar (ATCC CCL-185), H358 bronchioalveolar (ATCC CRL-5807), and NCI-H441 [H441] (ATCC HTB-174) were purchased from the American Type Culture Collection ATCC (Manassas, Virginia). Dulbecco's modified Eagle's medium advanced 1× (DMEM), RPMI-1640 medium, fetal bovine serum (FBS), Pen-Strep, Fungizone, Gentamicin, Insulin, Dexamethasone, and L-glutamine were obtained from Gibco by Life Technologies (Thermo Fisher Scientific Inc., Waltham, Massachusetts). SmallAir is a 3D human small airway epithelium reconstituted in vitro and its SmallAir special growth media (which is serum free and contains growth factors and phenol red) were both purchased from Epithelix (Geneva, Switzerland).
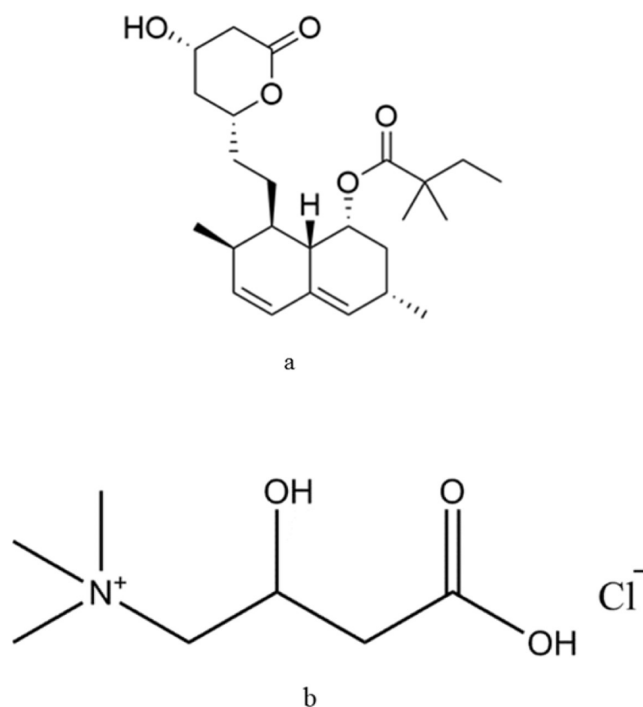
Figure 1. Chemical structures (ChemDraw Ultra Ver. 15.0.; CambridgeSoft, Cambridge, MA) of (a) Sim and (b) L-Car HCl.

METHODS

Preparation of Co-SD Particles by Organic Solution Advanced Cospray Drying in Closed-Mode

As previously reported,[15,19,25,26] organic solution advanced cospray drying processing in the absence of water was performed in the closed-mode using a Büchi B-290 mini Spray Dryer with a high-performance cyclone in the close mode using UHP dry nitrogen gas as the atomizing and the drying gas and connected to the B-295 Inert Loop (Büchi Labortechnik AG, Flawil, Switzerland). The starting feed solutions were prepared by dissolving the components in methanol to make two different total powder concentration solutions of 0.5% (w/v) and 1% (w/v). A Branson 7500 ultrasonicator was employed to assist with the dissolution. Table 1 lists the SD conditions. The drying gas atomization

Table 1. SD Conditions for Co-SD Sim:L-Car HCl Systems

spray drying conditions	
T_{Inlet}	150 °C
aspirator rate	100% (35 m³/h)
pump rate	25% (7.5 mL/min)
gas flow	55 mm (670 L/h)
feed solution concentration	0.5% w/v, 1% w/v
solvent	methanol
atomizing and drying gas	UHP nitrogen
nozzle type diameter	stainless steel (0.7 mm)

rate (670 L/h at 35 mm Hg), the aspiration rate (35 m³/h at 100% rate), and the inlet temperature (150 °C) were maintained constant during all the experiments. The corresponding outlet temperatures are listed in Table 2. The stainless-steel nozzle diameter was 0.7 mm. The Co-SD particles were separated from the nitrogen drying gas in the high-performance cyclone and collected in the small sample collector. All Co-SD powders were carefully stored in sealed glass vials and stored in sealed glass desiccators over Indicating Drierite/Drierite desiccant at −20 °C.

Table 2. SD Outlet Temperatures and Residual Water Content for Co-SD Sim:L-Car HCl Systems

Co-SD Sim:L-Car HCl system molar ratio compositions	T_{Outlet} (°C)	residual water content (% w/w)
0.5% w/v Sim:L-Car Feed Concentration		
50:50	75−82	8.44 ± 0.40
60:40	76−78	6.68 ± 1.37
75:25	75−80	7.04 ± 0.39
80:20	84−87	4.19 ± 0.43
1% w/v Sim:L-Car HCl Feed Concentration		
50:50	80	7.80 ± 2.61
60:40	75−75	5.21 ± 0.24
75:25	68−70	5.29 ± 0.77
80:20	75−78	3.70 ± 0.27

Scanning Electron Microscopy and Energy-Dispersive X-ray Spectrometry

Visual imaging and analysis of particle characteristics were observed by scanning electron microscopy (SEM) using a FEI Inspect S microscope (FEI, Brno, Czech Republic), as previously reported.[15,19,25,26] Briefly, samples were placed on double-sided adhesive carbon tabs (TedPella, Inc.) which were adhered to aluminum stubs (TedPella, Inc.) and were coated with a gold/palladium alloy thin film using a Hummer VI sputtering system from Technics. The coating process was operated at 10 AC mA for 3 min. The electron beam with an accelerating voltage of 20 kV was used at a working distance of 30 mm. Energy-dispersive X-ray (EDX) was performed using ThermoNoran systems Six (Thermo Scientific, Waltham, Massachusetts) at an accumulation voltage of 30,000 eV, the spot size was increased until a dead time of 20−30 was obtained.[15,19,25,26]

Particle Sizing and Size Distribution Using SEM Micrographs

SigmaScan Pro 5.0.0 (Systat, Inc., San Jose, California) was used to get the mean size, standard deviation, and size range of the particles based on their scanning electron micrographs using a similar procedure that we had previously reported.[9,15,19,26] The number of particles per measurements was ≥100 particles.

Karl Fisher Titration

Approximately 2−10 mg of powder was added to the titration cell containing Hydranal Coulomat AD reagent, and the residual water content was calculated using a TitroLine 7500 trace titrator (SI Analytics, Weilheim, Germany), as previously reported.[15,19,25,26]

X-ray Powder Diffraction

Using conditions similar to previously reported,[15,19,25,26] X-ray powder diffraction (XRPD) patterns of the different systems were obtained using a PANalytical X'pert diffractometer (PANalytical Inc., Westborough, Massachusetts) equipped with a programmable incident beam slit and an X'Celerator Detector. Measurements were taken between 5.0 and 60.0° (2θ) with a scan rate of 2°/min.

Differential Scanning Calorimetry

Using conditions similar to previously reported,[15,19,25,26] thermal analysis and phase transition measurements were conducted on a TA Q1000 differential scanning calorimeter (DSC) (TA Instruments, New Castle, Delaware) equipped with T-Zero technology, RSC90 automated cooling system, auto sampler, and calibrated with indium. Hermetic sealed T-Zero pans (TA Instruments, New Castle, Delaware) and T-Zero lids (TA Instruments, New Castle, Delaware) were used. The samples were heated from at least 0.00 to 250.00 °C at a scanning rate of 5.00 °C/min. All measurements were carried out in triplicate (n = 3).

Hot Stage Microscopy under Cross-Polarizers

Using conditions similar to those previously reported,[15,19,25,26] hot-stage microscopy (HSM) was performed using a Leica DMLP cross-polarized microscope (Wetzlar, Germany) equipped with a Mettler FP 80 central processor heating unit and a Mettler FP82 hot stage (Columbus, Ohio). Samples were mounted on a glass slide and heated from at least 25.0 to 250.0 °C at a heating rate of 5.00 °C/min.

ATR-FTIR Spectroscopy

Molecular fingerprinting by attenuated total reflectance Fourier transform infrared (ATR-FTIR) spectroscopy was obtained using a Nicolet Avatar 360 FTIR spectrometer (Varian Inc., California) equipped with a DTGS detector and a Harrick MNP-Pro (Pleasantville, New York) ATR accessory. Spectral data were acquired with EZ-OMNIC software under conditions similar to our previous reports.[15,19,25,26]

In Vitro Aerosol Dispersion Performance

In accordance with USP Chapter ⟨601⟩ specifications on aerosols[27] and using conditions similar to those previously reported,[15,19,25,26] the in vitro aerosol dispersion performance of the Co-SD particles was tested using the stainless steel Next Generation Impactor (NGI) (MSP Corporation, Shoreview, Minnesota) with a stainless steel induction port (USP throat) attachment (NGI model 170; MSP Corporation) equipped with specialized stainless steel NGI gravimetric insert cups (MSP Corporation, Minneapolis, MN). Two FDA-approved human DPI devices with varying shear stress properties: the HandiHaler (Boehringer Ingelheim, Ingelheim, Germany), which is a high shear stress human DPI device,[6,28] and the NeoHaler (Novartis AG, Stein, Switzerland), which is a medium sheer stress human DPI device, were used.[6,29] An airflow rate (Q) of 60 L/min, which is the adult airflow rate and standard airflow rate for DPI testing, was adjusted and measured before each experiment using a Copley DFM 2000 digital flow meter (Copley Scientific, Nottingham, United Kingdom). The NGI was connected to a Copley HCP5 high-capacity vacuum pump (Copley Scientific, Nottingham, United Kingdom) through a COPLEY TPK 2000 critical flow controller (Copley Scientific, Nottingham, United Kingdom). The mass of powder deposited on each NGI gravimetric cup stage was quantified by a gravimetric method using type A/E glass fiber filters with diameters of 55 mm (PALL Corporation, Port Washington, New York) and 75 mm (Advantec, Japan). Quali-V clear HPMC size 3 inhalation grade capsules (Qualicaps, North Carolina) were each filled with ∼10 mg of powder. Three capsules were used in each experiment. In vitro aerosolization was evaluated in triplicate (n = 3) under ambient conditions.

For the NGI, Q = 60 L/min, the D_{a50} aerodynamic cutoff diameter for each NGI stage was calibrated by the manufacturer and stated as follows: stage 1 (8.06 μm); stage 2 (4.46 μm); stage 3 (2.82 μm); stage 4 (1.66 μm); stage 5 (0.94 μm); stage 6 (0.55 μm); and stage 7 (0.34 μm). The emitted dose (ED) was determined as the difference between the initial mass of powder loaded in the capsules and the remaining mass of powder in the capsules following aerosolization. The ED (%) eq 1 was used to express the percentage of ED based on the total dose (TD) used. The fine particle dose (FPD) was defined as the dose deposited on stages 2−7. The fine particle fraction (FPF %) eq 2 was expressed as the percentage of FPD to ED. The respirable fraction (RF %) eq 3 was used as the percentage of FPD to total deposited dose (DD) on all impactor stages.

$$\text{Emitted dose fraction (ED \%)} = \frac{\text{ED}}{\text{TD}} \times 100\% \tag{1}$$

$$\text{Fine particle fraction (FPF \%)} = \frac{\text{FPD}}{\text{ED}} \times 100\% \tag{2}$$

$$\text{Respirable fraction (RF \%)} = \frac{\text{FPD}}{\text{DD}} \times 100\% \tag{3}$$

In addition, the mass median aerodynamic diameter (MMAD) of aerosol particles and geometric standard deviation (GSD) were calculated using a Mathematica (Wolfram Research, Inc., Champaign, Illinois) program written by Dr. Warren Finlay.

In Vitro Viability Assay in a 2D Cell Culture

The effects Co-SD formulations on cell proliferation were analyzed by measuring the response of lung adenocarcinoma and bronchoalveolar

a.

b.

c.

d.
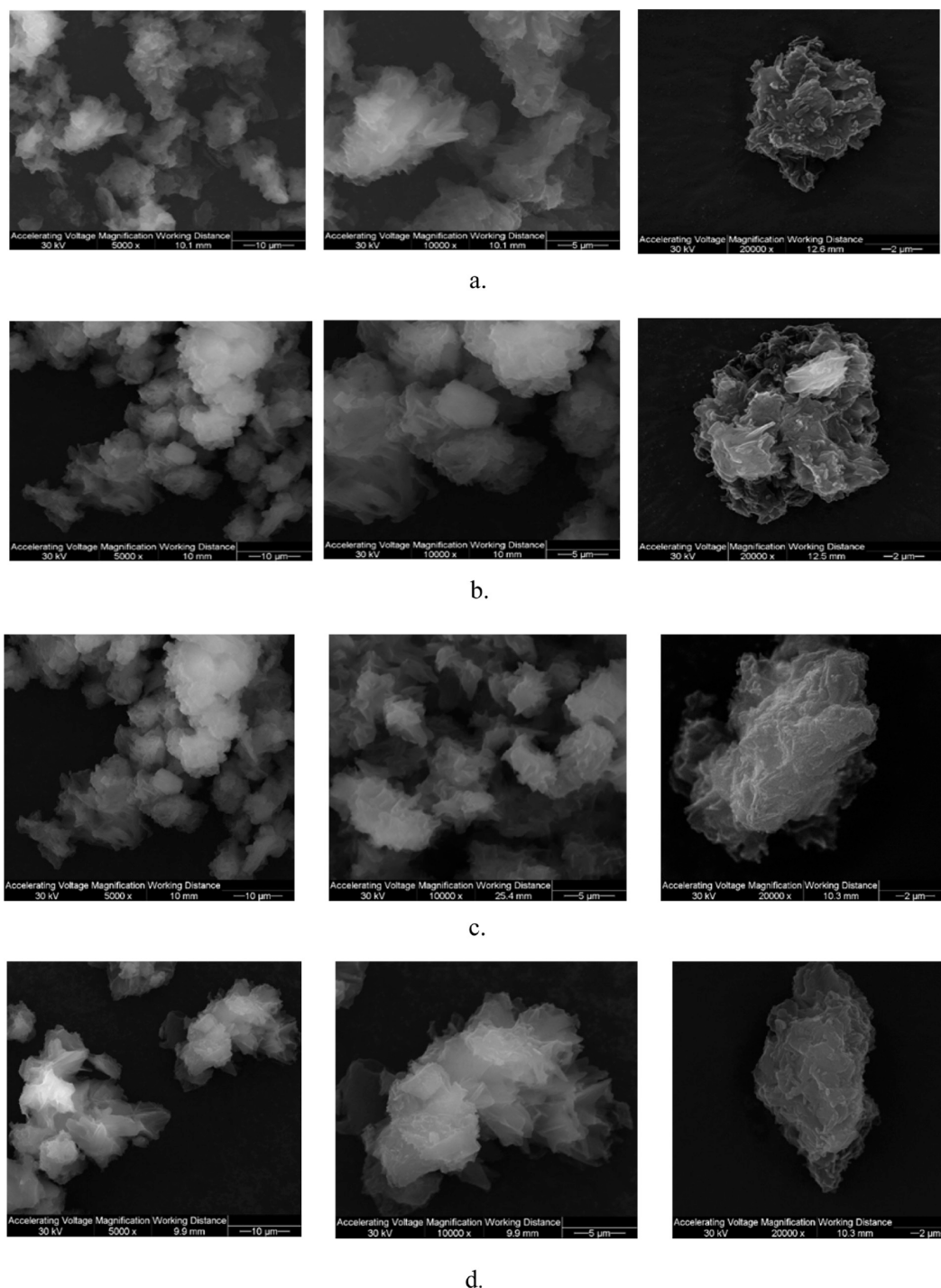
Figure 2. SEM micrographs of (a) 0.5% w/v Co-SD 50:50 Sim:L-Car HCl; (b) 0.5% w/v Co-SD 60:40 Sim:L-Car HCl; (c) 0.5% w/v Co-SD 75:25 Sim:L-Car HCl; and (d) 0.5% w/v Co-SD 80:20 Sim:L-Car HCl.

carcinoma cells (A549 and H358, respectively) to different concentrations of the Co-SD powders. Cell lines were grown in similar conditions, as described in previously.[9,15,19,30,31]

A549 and H358 cells were seeded in 96-well plates at 5000 cells/well and 100 μL/well and were allowed 48 h to attach. The cells were then exposed to different concentrations of the Co-SD formulations. The powders were dissolved in 10% ethanol and 90% DMEM media. A volume of 100 μL of this drug solution were added to each well. Seventy-two hours after exposure, a volume of 20 μL of 20 μM resazurin sodium salt were added to each well and incubated for 4 h. At this point, the fluorescence intensity of the resorufin (fluorescent metabolite) produced by viable cells was detected at 544 nm (excitation) and 590

nm (emission) using the Synergy H1 Multi-Mode Reader (BioTek Instruments, Inc., Winooski, VT). The relative viability of cell line was calculated as followed by eq 4

$$relative\ viability\ (\%) = \frac{sample\ fluorescence\ intensity}{control\ fluorescence\ intensity} \times 100\%$$

(4)

In vitro transepithelial electrical resistance on 2D human lung epithelial cells at the air−liquid interface

The NCI-H441 cell line was grown in T-75 culture flasks in an atmosphere of 5% CO_2 at 37 °C. H441 cells were maintained in a proliferation medium (RPMI 1640-Gibco) containing 10% FBS, 1%
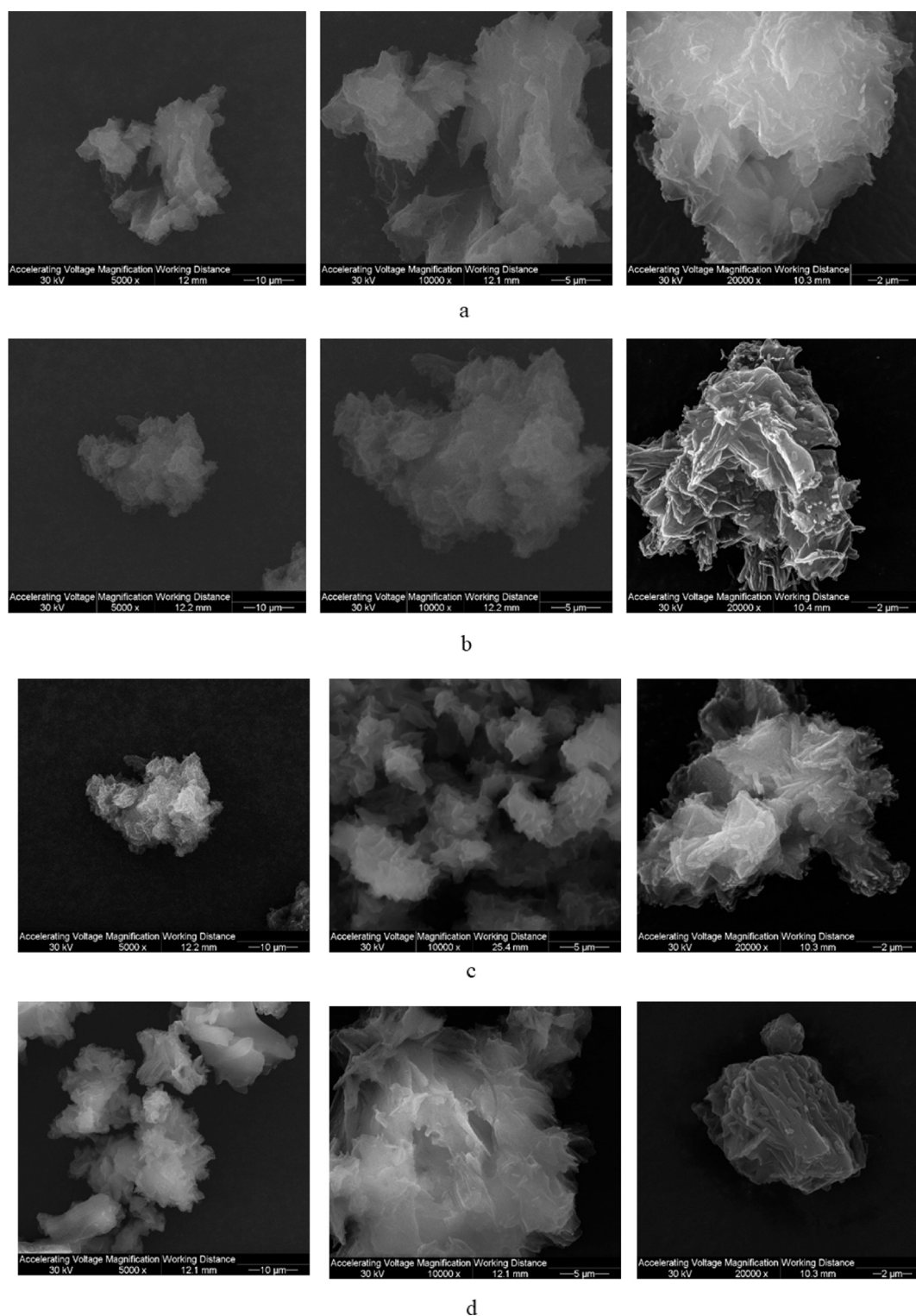
Figure 3. SEM micrographs of (a) 1% w/v Co-SD 50:50 Sim:L-Car HCl; (b) 1% w/v Co-SD 60:40 Sim:L-Car HCl; (c) 1% w/v Co-SD 75:25 Sim:L-Car HCl; and (d) 1% w/v Co-SD 80:20 Sim:L-Car HCl.

penicillin−streptomycin (P/S), and 1% of GlutaMAX. Once they were confluent (90%), cells were seeded onto 12-well Transwell inserts (Costar 3460, Corning, New York) at a density of 250,000 cells/well in the proliferation medium (0.5 mL in the apical and 1.5 mL in the basolateral chambers). The seeding day was defined as day 0. Cells were allowed to attach before the medium was changed to a polarization medium. The basal media were changed every other day until the formation of a monolayer. Once the monolayer was formed, cells were

now fed with a polarization medium, which was made up of base medium RPMI 1640 containing 4% FBS, 1% penicillin−streptomycin, 1% GlutaMAX, 1% insulin-transferrin-selenium (Thermo Fisher, Waltham Massachusetts), and 200 nM dexamethasone (Sigma, St. Louis, Missouri). Three days later, the polarization medium was removed from the apical compartment, leaving the apical surface of the cells exposed to air (air liquid interface culture ALI). The medium was changed every two days. The maximum ALI TEER value expected was
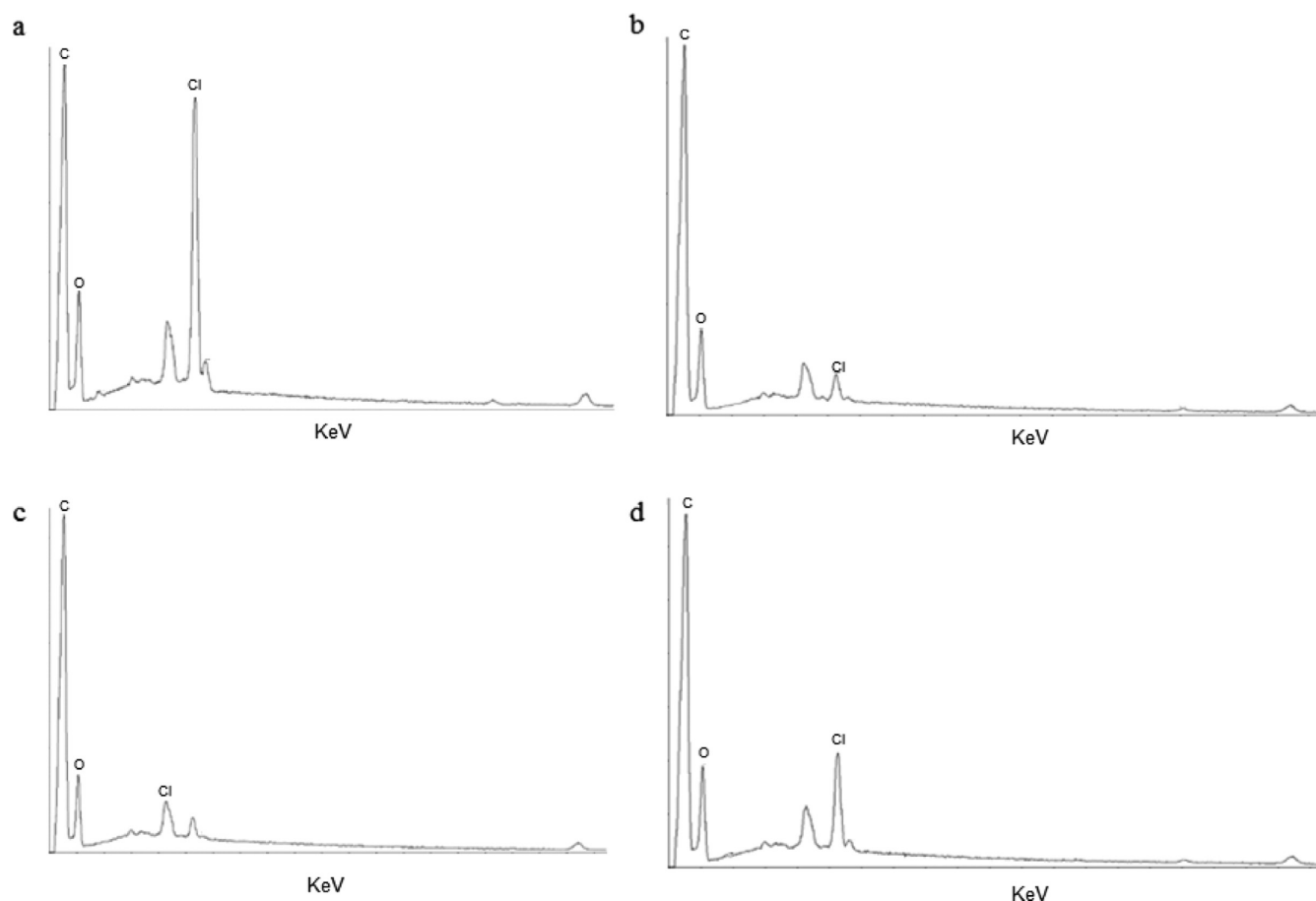
Figure 4. EDX spectra of (a) 1% w/v Co-SD 50:50 Sim:L-Car HCl; (b) 1% w/v Co-SD 60:40 Sim:L-Car HCl; (c) 1% w/v Co-SD 75:25 Sim:L-Car HCl; and (d) 1% w/v Co-SD 80:20 Sim:L-Car HCl.

around 250 Ω·cm². Once they reached that value, cells were exposed to the drug formulations. TEER values were read after 3 h of treatment and every day to monitor the behavior of the monolayer. An EndOhm 12 mm Culture Cup (World Precision Instruments, Sarasota, Florida) was utilized to measure the TEER of the cells. For TEER measurement, 0.5 mL of media was added to the apical side of the transwells 5 min before measurement and then immediately removed to return the cells to ALI conditions. This methodology was previously reported.[9,15,19,30−33]

In Vitro Cell-Dose Response Assay in 3D Human Small Airway Epithelia Cultures

The small airway epithelia reconstituted in vitro is built using primary small airways human cells which are fully differentiated and functional. Using similar conditions that we reported previously,[15,19,31] the cells were received in 24-well transwell inserts in an agar gel matrix. Once we received, we transferred them into a new 24-well plate with 700 μL of the SmallAir media in the basal side. Media were changed every other day.

After 3 days of incubation at 37 °C and 5% of CO₂, experiments were performed. For in vitro cell dose response, the cells were exposed to different concentrations of the drug formulation dissolved in 90:10 media/ethanol to facilitate dissolution. After 72 h of incubation, the inserts were rinsed with a 6 μM Resazurin solution in order to eliminate the remaining red phenol from the cell growth media. The inserts were transferred to a new 24 well plate filled will 500 μL/well of resazurin solution. 200 μL/well were added in the apical surface. After 1 hour of incubation, 100 μL from the apical side were transferred to a 96 black-well plate. At this point, the fluorescence intensity of the resorufin (fluorescent metabolite) produced by viable cells was detected at 544 nm (excitation) and 590 nm (emission) using the Synergy H1 Multi-Mode Reader (BioTek Instruments, Inc., Winooski, Vermont). The relative viability of the cell line was calculated as followed by eq 4. This

protocol was provided by the vendor[34] and used in our recent reports.[15,19,31]

In vitro TEER in 3D human small airway epithelia cultures at the ALI.

As described above and in our recent reports,[15,19,31] after receiving the cells, they were transferred to a new 24-well plate prefilled with 700 μL of SmallAir media in the basal side. After 3 days of incubation, the experiments were performed. TEER values were obtained before exposure to the drug solution, 3 h after exposure and then every 24 h for 5 days. To measure TEER, 200 μL of the cell media was added to the apical surface of the inserts. TEER values were measured using EVOMX (Epithelial VoltohmMeter) and electrode (STX2) (World Precision Instruments, Sarasota, FL). The long part of the electrode was inserted through the gap of the insert and leaned on the bottom of the well, and the short stem was above in the apical surface, inside the culture media. Every time the TEER measurement was finished, the media were removed from the apical surface in order to leave the cells in ALI conditions. This was followed by the protocol given by the vendor[34] and used in our recent reports.[15,19,31]

Statistical Analysis

Design of experiments (DoEs) was conducted using Design-Expert 8.0.7.1 software (StatEase Corporation, Minneapolis, MN). A multi-factorial DOE for the Co-SD powders was utilized for in vitro aerosol testing. The different interaction parameters on the performance of the formulations were evaluated using 3-D surface plot analyses generated from Design-Expert 8.0.7.1 software (StatEase Corporation, Minneapolis, MN). All experiments were performed in triplicate ($n = 3$). Results were expressed as mean ± standard deviation.

■ RESULTS

Scanning Electron Microscopy

Size and morphology of raw and Co-SD particles were visualized by SEM, and their micrographs are shown in Figures 2 and 3 for 0.5% (w/v) and 1% (w/v), respectively. Co-SD systems were attained at SD liquid feed concentrations of 0.5% (w/v) and 1% (w/v). The Sim:L-Car molar ratios were 50:50, 60:40, 75:25, and 80:20. The SD pump rate (PR) was fixed at 25% PR. Other PRs were tested but no particles were produced. All Co-SD systems showed that the particles were irregularly shaped with rough surfaces, rather than spherical. These surface features are known to influence aerosolization performance, potentially reducing particle agglomeration and improving dispersibility in the DPI. Formation of aggregates were shown in the micrographs; therefore, it was hard to distinguish single particles. Figure 4 showed the EDX spectra of all Co-SD powder systems, where the Cl atom was present in all powders after SD. The peak for the 50:50 system was much higher than the peaks of all the other systems.

Particle Sizing and Size Distribution by Image Analysis of SEM Micrographs

As listed in Table 3, all Co-SD systems had about the same geometric mean diameters. All of them were around 7 μm $\pm$

Table 3. Particle Sizing Using Image Analysis on SEM Micrographs ($n \geq 100$ Particles)

Co-SD Sim:L-Car system molar ratio compositions	mean size $\pm$ standard deviation (μm)	range (μm)
0.5% w/v Sim:L-Car Feed Concentration		
50:50	7.12 $\pm$ 3.02	2.01−19.38
60:40	7.5 $\pm$ 2.61	2.91−14.83
75:25	7.5 $\pm$ 2.77	2.3−16.74
80:20	9.26 $\pm$ 4.2	3.03−24.05
1% w/v Sim:L-Car Feed Concentration		
50:50	7.36 $\pm$ 2.99	2.72−16.68
60:40	7.47 $\pm$ 3.08	3.45−20.14
75:25	7.11 $\pm$ 3.3	2.33−22.79
80:20	8.12 $\pm$ 2.73	2.84−15.34

standard deviation. The ranges varied between systems, but the low values were ∼2−3 μm for all systems, whereas the high values were ∼16−24 μm for all systems.

Karl Fisher Titration

The residual water content of raw Sim, raw Car, SD Sim, and SD L-Car one-component powders were recently reported by us.[15,19] The residual water content for Co-SD Sim:L-Car powders was quantified by KFT. Residual water content values are listed in Table 2. Co-SD 50:50 molar ratio systems had more residual water content than the other systems. The residual water content decreased by increasing the amount of Sim in the Co-SD powders. The starting feed solution concentration did not affect the KFT values. In general, the residual water content of all Co-SD systems were in the range of 3.7%−8.5% w/w.

X-ray Powder Diffraction

The diffractograms of raw and one-component SD Sim and L-Car powders have been recently reported by us.[15,19] As shown in Figure 5, the diffractograms of all Co-SD powders showed sharp peaks reflective of long-range molecular order which are indicative of crystallinity in the solid-state. Sharp peaks were

seen for all 0.5% (w/v) and 1% (w/v) Co-SD systems. All Co-SD systems showed characteristic peaks of Sim and L-Car.

Differential Scanning Calorimetry

The thermograms of raw and one-component pure Sim and L-Car powders were reported recently by us.[15,19] The thermograms of Co-SD systems (0.5% (w/v) and 1% (w/v)) are shown in Figures 6 and 7, respectively. All Co-SD systems showed similar thermograms. There was one endothermic first-order phase transition evident, which corresponded to the solid-to-liquid melting of the powder between 118 and 126 °C in all systems. Fast DSC heating scans were conducted at 20 and 40 °C/min for all systems; however, no second-order glass transition temperature (T_g) was detected (data not shown). Phase transition temperatures and enthalpies for all systems are summarized in Table 4.

HSM Under Cross-Polarizer Lens

Representative images from HSM for both feed solution concentrations are presented in Figure 8. The HSM for raw Sim, raw L-Car HCL, SD Sim, and SD L-Car HCL one-component powders were reported recently by us.[15,19] The Co-SD systems exhibited birefringence under the cross polarized light. This confirmed the crystallinity observed in XRPD diffractograms. There was not any visible minor phase transition in the HSM images. The melting point was clearly observed in both systems at ∼120 °C, which was very similar to the melting in the DSC thermograms.

Attenuated Total Reflectance Fourier Transform Infrared Spectroscopy

The ATR-FTIR molecular fingerprinting spectra of raw Sim, raw L-Car HCl, SD Sim, and SD L-Car HCL powders were reported earlier by us.[15,19] ATR-FTIR molecular fingerprinting spectra of Co-SD powders, shown in Figures 9 and 10, had representative peaks at 2950, 1840, 1770, 1650, 1260, and 1160 cm^{-1}. Sharp peaks at 1840 and 1770 cm^{-1} are characteristic of C=O stretching from the ester and lactone groups of Sim, confirming the presence of carbonyl group. A peak at 1650 cm^{-1} indicates C=C stretching, which could be associated with the aromatic rings of Sim. Furthermore, the peaks at 1260 and 1160 cm^{-1} correspond to C−O stretching vibrations, likely from ester and hydroxyl groups and together, these peaks confirm the molecular integrity of the excipient-free Co-SD powder formulation drugs.

In Vitro Aerosol Dispersion Performance

In vitro aerosol dispersion performance (Figure 11) was successfully done using NGI. The comprehensive aerosol dispersion performance parameters for all Co-SD systems are listed in Table 5. The aerosol performance of one-component SD Sim and one-component SD L-Car DPI powder were recently reported by our group.[15,19] In general, all powders had ∼100% of the dose emitted from both devices tested. The FPF and RF values were higher for the 0.5% w/v Co-SD systems and in general using the NeoHaler device. The 1% w/v Co-SD systems had lower FPF and RF values and in general the values were lower using the HandiHaler device. The 0.5% w/v systems had smaller MMAD values using the Neohaler device. The MMAD values for the 1% w/v Co-SD systems did not show the same trend. The aerodynamic diameters were smaller using the HandiHaler device. Figure 11 shows the mass deposition on each stage of the NGI. Almost all the powder was deposited on the first stage. It was observed that the 0.5% w/v system presented more deposition in further stages with both devices than the 1% w/v % system.
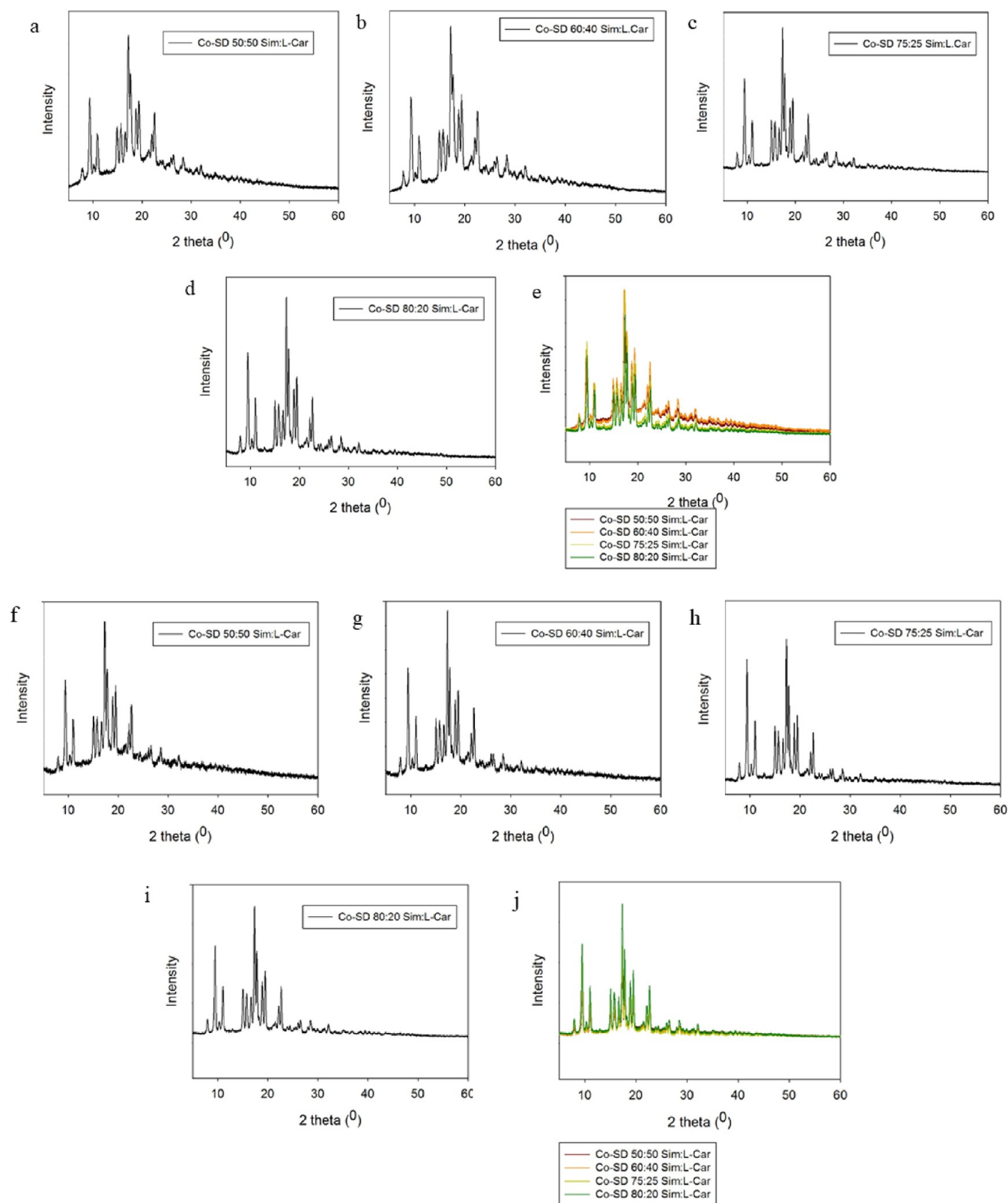
Figure 5. XRPD diffractograms of (a) 0.5% w/v Co-SD 50:50 Sim:L-Car HCl; (b) 0.5% w/v Co-SD 60:40 Sim:L-Car HCl; (c) 0.5% w/v Co-SD 75:25 Sim:L-Car HCl; (d) 0.5% w/v Co-SD 80:20 Sim:L-Car HCl; (e) all; (f) 1% w/v Co-SD 50:50 Sim:L-Car HCl; (g) 1% w/v Co-SD 60:40 Sim:L-Car HCl; (h) 1% w/v Co-SD 75:25 Sim:L-Car HCl; (i) 1% w/v Co-SD 80:20 Sim:L-Car HCl; and (j) all.

In Vitro Viability Assay in a 2D Cell Culture

As seen in Figure 12, after 72 h of exposure to different concentrations of the Co-SD systems, both cell lines (H358 and A549) remained safe (i.e., no decrease in viability). There was a minimum decrease in the viability of the cells after the exposure to the maximum tested concentration (100 μg/mL). At all other concentrations, the percentage of viability persisted close to
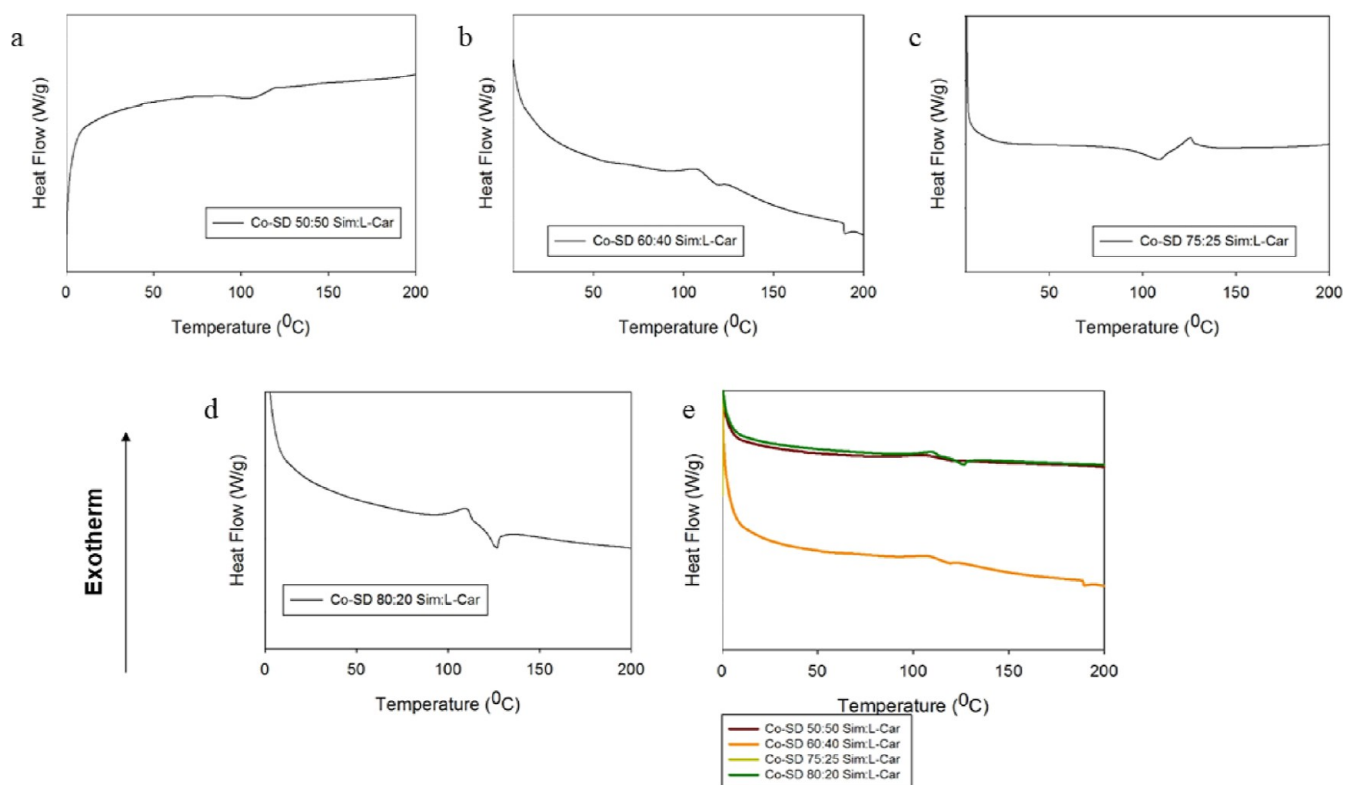
Figure 6. DSC thermograms of powders: (a) 0.5% w/v Co-SD 50:50 Sim:L-Car HCl; (b) 0.5% w/v Co-SD 60:40 Sim:L-Car HCl; (c) 0.5% w/v Co-SD 75:25 Sim:L-Car HCl; (d) 0.5% w/v Co-SD 80:20 Sim:L-Car HCl; and (e) all.
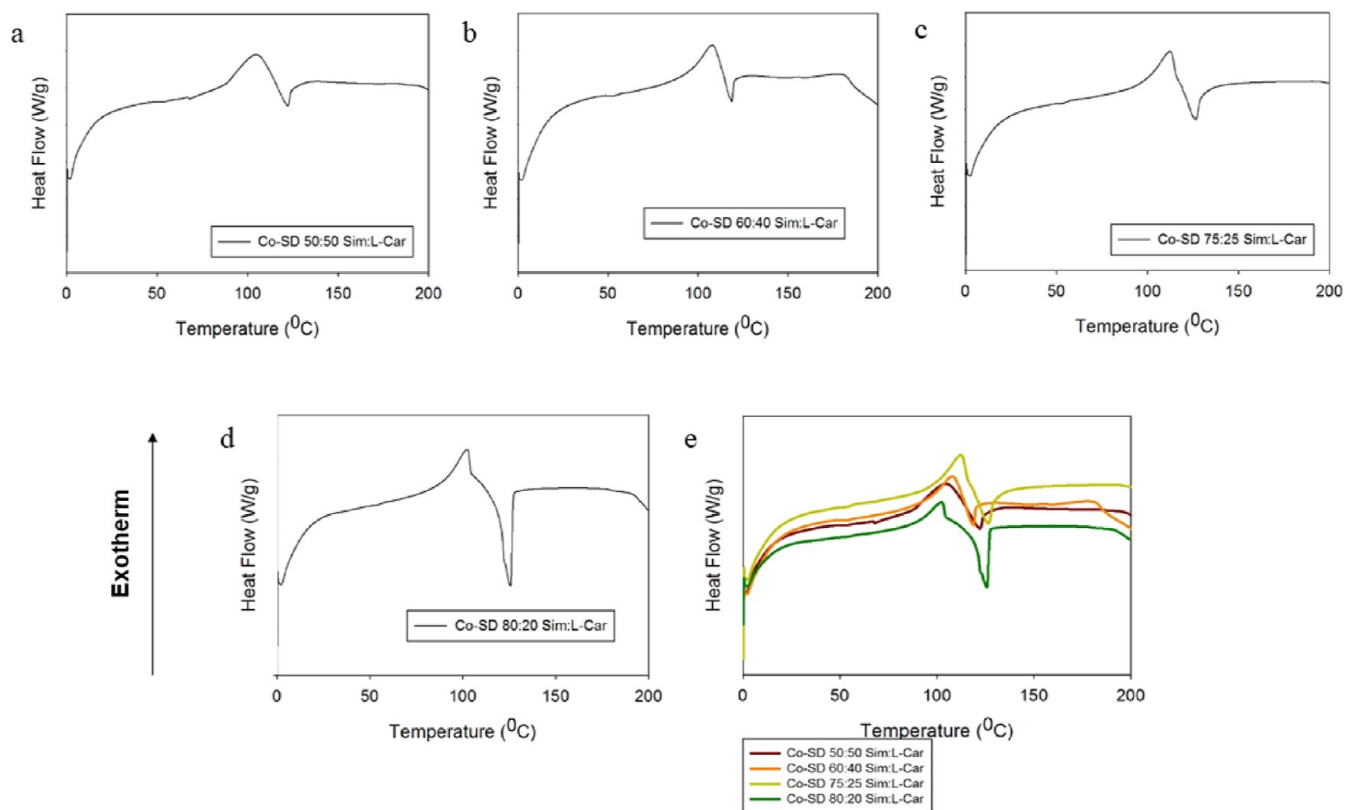
Figure 7. DSC thermograms of powders: (a) 1% w/v Co-SD 50:50 Sim:L-Car HCl; (b) 1% w/v Co-SD 60:40 Sim:L-Car HCl; (c) 1% w/v Co-SD 75:25 Sim:L-Car HCl; (d) 1% w/v Co-SD 80:20 Sim:L-Car HCl; and (e) all.

Table 4. Solid-State Phase Transition Temperature (T_{peak}) and Enthalpy (ΔH) Values for Co-SD Sim:L-Car HCl Dry Powders (n = 3, Mean $\pm$ SD)

Co-SD Sim:L-Car HCl powders molar ratio compositions	T_{peak} (°C)	enthalpy (ΔH) (J/g)
0.5% w/v Sim:L-Car HCl Feed Concentration		
50:50	123.13 $\pm$ 2.70	28.34 $\pm$ 6.64
60:40	119.93 $\pm$ 1	22.65 $\pm$ 3.78
75:25	123.53 $\pm$ 33.71	33.71 $\pm$ 14.67
80:20	125.75 $\pm$ 0	54.74 $\pm$ 0.38
1% w/v Sim:L-Car HCl Feed Concentration		
50:50	120.84 $\pm$ 3.11	14.96 $\pm$ 7.8
60:40	117.09 $\pm$ 2.34	9.45 $\pm$ 3.79
75:25	124.55 $\pm$ 1.17	23.95 $\pm$ 15.37
80:20	125.62 $\pm$ 2.34	24.23 $\pm$ 4.16

100% taking into consideration the standard deviations. In vitro cell viability dose effects of Sim and Car as one-component systems were recently reported by our group.[15,19]

In vitro TEER on 2D human lung epithelial cells at the ALI. After 100 μg/mL of exposure, the electrical resistance of H441 had a minimal decrease as it can be seen in Figure 13. Over time, the TEER kept increasing until it was about the same as it

was before the exposure to the formulations. In vitro TEER on 2D pulmonary cells at the ALI for Sim and Car as one-component systems were recently reported by our group.[15,19]

In Vitro Cell-Dose Response Assay in 3D Human Small Airway Epithelia Cultures

The relative viability of the SmallAir human small airway epithelia cultures after exposure to 1000 μg/mL of 1% w/v Co-SD 50:50 Sim:L-Car was 0%. After decreasing the concentration to 100 μg/mL, the relative viability increased to 63%, as shown in Figure 14. In vitro viability in 3D SmallAir as one-component systems were recently reported by our group.[15,19]

In Vitro TEER in 3D Human Small Airway Epithelia Cultures at the ALI

When cells were exposed to 1000 μg/mL solution of 1% w/v Co-SD 50:50 Sim:L-Car, the membrane was irreversibly disrupted. TEER values at the ALI were below 100 Ω/cm^2 after the exposure and they never recovered (i.e., irreversible membrane disruption). On the other hand, when the concentration was decreased to 100 μg/mL, the values were above 200 Ω/cm^2, as shown in Figure 15. In vitro TEER on 3D human small airway epithelia cultures at the ALI for Sim and Car
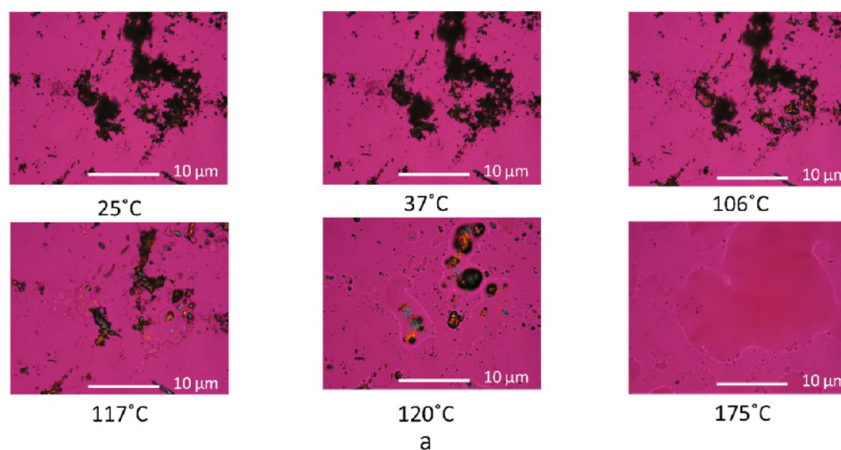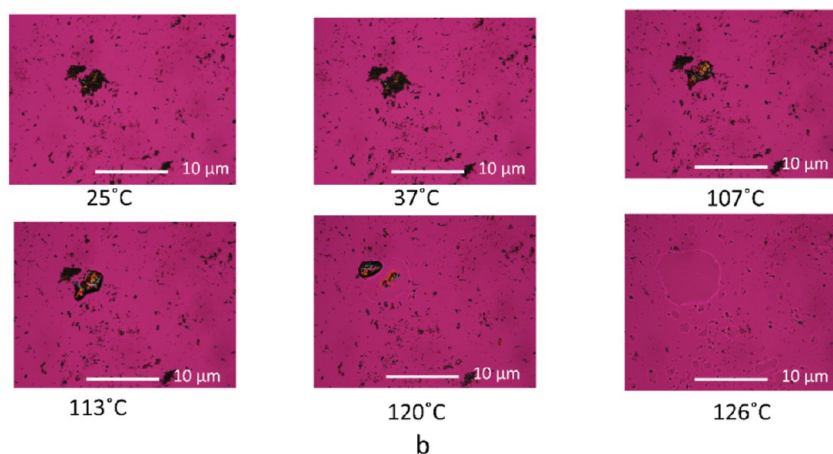
Figure 8. HSM images at different temperatures of (a) 0.5% w/v Co-SD 75:25 Sim:L-Car HCl and (b) 1% w/v Co-SD 80:20 Sim:L-Car HCl. Scale bar = 10 μm.
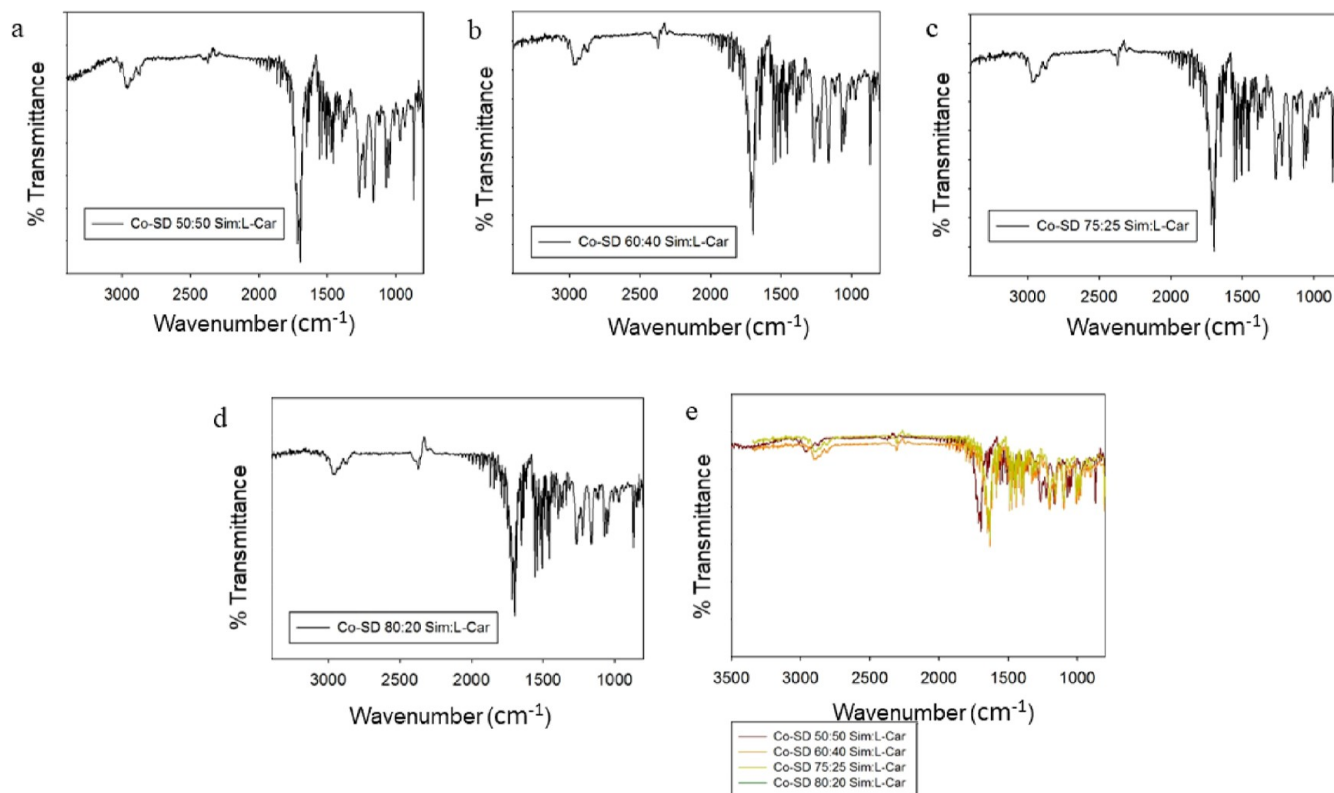
Figure 9. ATR-FTIR spectra of (a) 0.5% w/v Co-SD 50:50 Sim:L-Car HCl; (b) 0.5% w/v Co-SD 60:40 Sim:L-Car HCl; (c) 0.5% w/v Co-SD 75:25 Sim:L-Car HCl; (d) 0.5% w/v Co-SD 80:20 Sim:L-Car HCl; and (e) all.
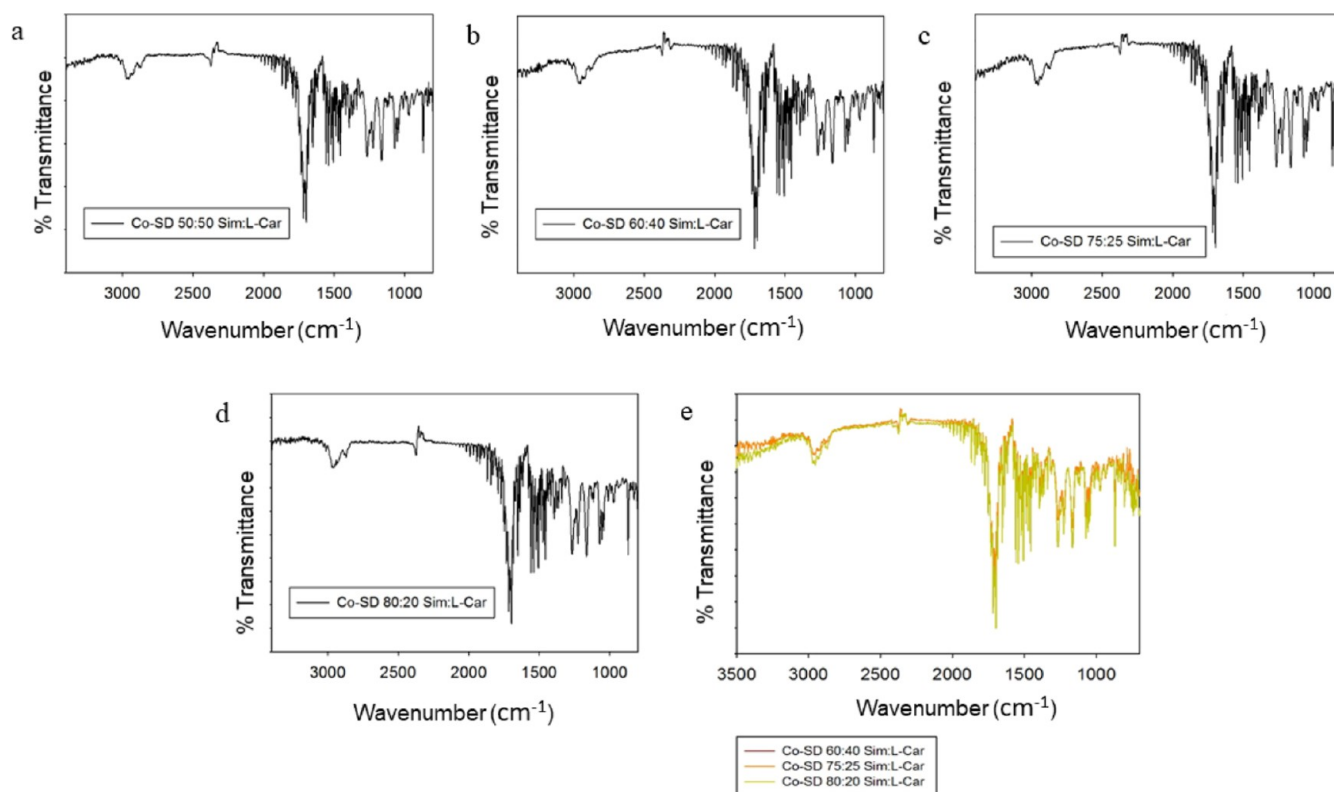
Figure 10. ATR-FTIR spectra of (a) 1% w/v Co-SD 50:50 Sim:L-Car HCl; (b) 1% w/v Co-SD 60:40 Sim:L-Car HCl; (c) 1% w/v Co-SD 75:25 Sim:L-Car HCl; (d) 1% w/v Co-SD 80:20 Sim:L-Car HCl; and (e) all.

as one-component systems were recently reported by our group.[15,19]
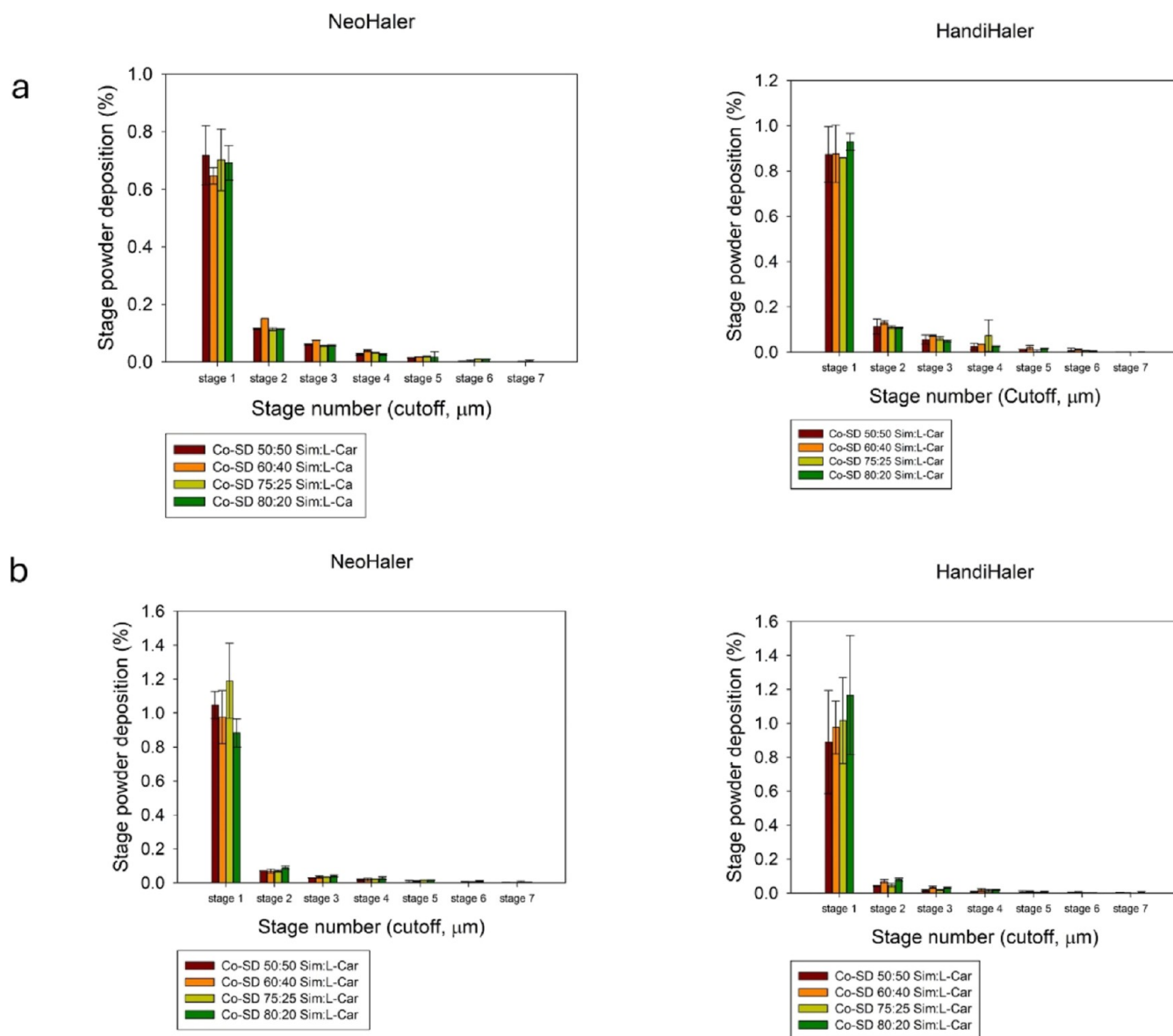
Figure 11. In vitro dry powder aerosol deposition of (a) 0.5% w/v Co-SD systems and (b) 1% w/v Co-SD systems.

■ DISCUSSION

To the authors' knowledge, this was the first time that the Nrf2 activator ROCK inhibitor, Sim, was successfully formulated in dual-drug combination with L-Car as a carrier-free DPI employing organic solution advanced closed-mode SD. The Co-SD systems of Sim with L-Car can synergistically ameliorate PH because of these components' pleiotropic and antioxidant molecular mechanistic effects. Wong et al.[35] delivered Sim intraperitoneally to neonatal rats, demonstrating therapeutic efficacy by blocking the RhoA/ROCK pathway, which is crucial in pulmonary artery remodeling and right ventricular hypertrophy in PH patients.

Decreasing the interparticulate interactions to a minimum could lead to high FPF values. Structural cohesion and aggregation due to interparticulate interactions such as van der Waals forces, capillary forces, electrostatic forces, and mechanical interlocking avoid the proper aerosolization of the powder, leading to low FPF values. Particle characteristics such as morphology, size, surface, and density, among others, which are theoretically of importance in the development of

therapeutic powder aerosol formulations can be manipulated depending on the desirable formulation and the parameters employed on SD.[36] In this study, the formation of particles was achieved at low PR (25%) in all the systems. Different molar ratios and two starting feed solutions were rationally designed in order to compare their physicochemical characteristics and their in vitro aerosol dispersion performance using two human FDA approved DPI devices.

Excipient-free DPIs are important because they can deliver pure APIs directly to the lungs without the use of extra stabilizers or carriers. This is especially beneficial for individuals who are sensitive or allergic to excipients, as it minimizes the possibility of adverse effects. Excipient-free formulations further ensure that the API's therapeutic action is neither damaged or diluted by nonactive ingredients, potentially increasing drug bioavailability and efficacy. The irregular and rough surface particles were achieved in all Co-SD systems as seen in SEM micrographs (Figures 2 and 3). Nanostructures were visible on the surface of the particles leading to their aggregation. It was clearly observed that where single particles could be identified, the size was much

Table 5. In Vitro Aerosol Dispersion Performance as a Function of Co-SD Sim:L-Car Powder Composition and Human DPI Device Type Using the NGI[a]

Co-SD Sim:L-Car HCl powders molar ratio compositions	ED (%)	FPF (%)	RF (%)	MMAD (μm)	GSD
0.5% w/v Sim:L-Car HCl (NeoHaler)					
50:50	100 ± 0	7.18 ± 0.42	23.33 ± 2.97	17.40 ± 1.82	2.94 ± 0.02
60:40	100 ± 0	9.54 ± 0.56	30.69 ± 1.58	13.48 ± 0.2	2.8 ± 0.12
75:25	100 ± 0	7.62 ± 0.01	24.9 ± 3.08	19.8 ± 3.04	3.64 ± 0.15
80:20	100 ± 0	12.13 ± 6.6	33.32 ± 10.71	20.38 ± 1.09	3.84 ± 0.12
0.5% w/v Sim:L-Car HCl (HandiHaler)					
50:50	100 ± 0	7.58 ± 3.38	19.89 ± 8.03	24.52 ± 6.69	3.51 ± 0.25
60:40	100 ± 0	8.78 ± 0.36	23.80 ± 2.49	20.33 ± 1.64	3.63 ± 0.15
75:25	100 ± 0	8.32 ± 2.14	22.75 ± 4.28	18.11 ± 5.15	3.19 ± 0.12
80:20	100 ± 0	6.86 ± 0.3	18.02 ± 06	33.12 ± 5.6	4.46 ± 0.78
1% w/v Sim:L-Car HCl (NeoHaler)					
50:50	100 ± 0	4.04 ± 0.16	10.6 ± 0.4	39.6 ± 6.21	3.66 ± 0.29
60:40	100 ± 0	4.55 ± 0.89	12.18 ± 0.52	44.24 ± 0.45	4.25 ± 0.5
75:25	100 ± 0	5.01 ± 0.12	11.3 ± 1.16	54.29 ± 10.37	4.82 ± 0.13
80:20	100 ± 0	6.15 ± 0.34	17.37 ± 0.2	41.75 ± 14.6	5.52 ± 1.80
1% w/v Sim:L-Car HCl (HandiHaler)					
50:50	100 ± 0	2.47 ± 0.28	8.44 ± 3.4	46.54 ± 19.76	3.2 ± 0.42
60:40	100 ± 0	3.66 ± 0.03	8.7 ± 0.36	30.33 ± 3.15	5.61 ± 1.68
75:25	100 ± 0	2.85 ± 0.36	8.04 ± 2.91	54.28 ± 2.91	4.57 ± 0.83
80:20	100 ± 0	5.06 ± 0.03	11.54 ± 3.66	33.5 ± 2.14	4.36 ± 1.3

[a]MMAD, GSD, FPF, RF, and ED (n = 3, mean ± SD).

a.

b.
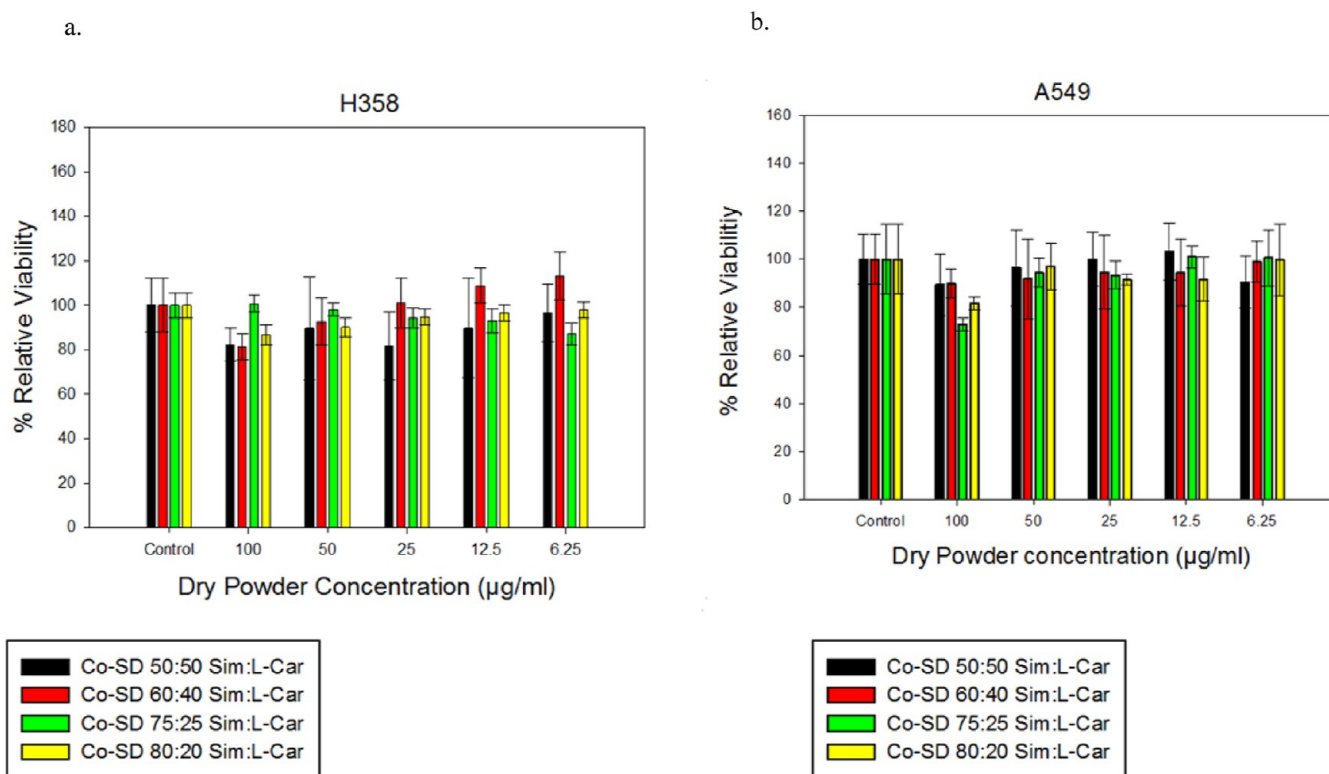
Figure 12. In vitro cell viability plots for (a) H358 human bronchioalveolar and (b) A549 human alveolar cells after 72 h of exposure to different concentrations of Co-SD Sim-L-Car HCl systems (n = 6, mean ± SD).

smaller than on the aggregates. The ED was ~100% even though SEM micrographs showed aggregation of the particles. Nair and Smyth (2023)[37] reported on excipient-free tigecycline DPI particles, both unmilled and milled. Using SD conditions and SD parameters different from reported in this study, Quarta et al. (2020)[38] reported on excipient-free insulin spray-dried powder

for inhalation using open-mode SD of water/ethanol cosolvent feed solutions different.

Most of the powder was deposited on the first stage of the NGI; however, there was also measurable powder on the lower stages (Figure 11). This gave comparable FPF and RF values with what is currently on the market.[9] Even though particles were forming aggregates, the interparticulate forces were not
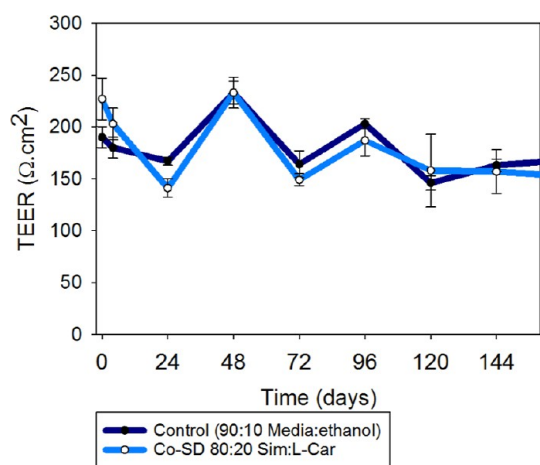
Figure 13. In vitro TEER analysis of H441 lung epithelial cells exposed to 100 μg/mL Co-SD Sim:L-Car in ALI culture conditions ($n = 3$, mean ± SD).
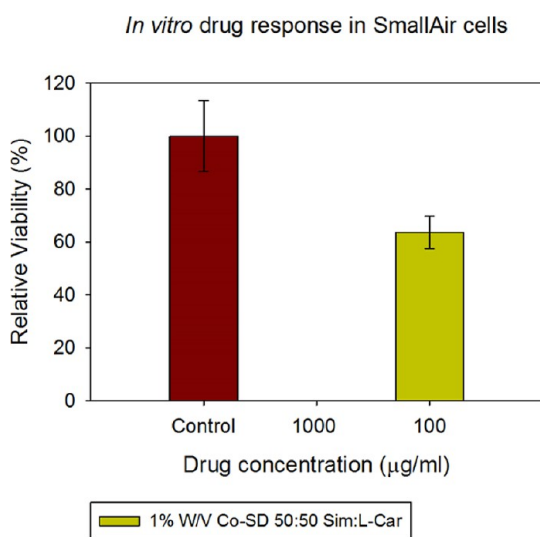
Figure 14. In vitro cell viability plots for SmallAir cells after 72 h of exposure to different concentrations of the Co-SD 50:50 Sim-L-Car HCl system ($n = 6$, mean ± SD).
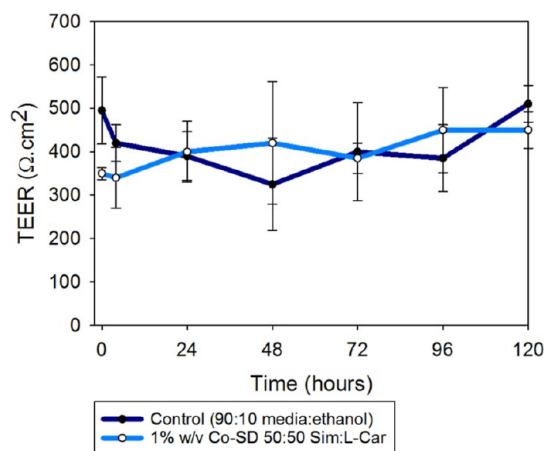
Figure 15. In vitro TEER analysis of SmallAir 3D human small airway epithelia exposed to 100 μg/mL Co-SD 50:50 Sim:L-Car HCl in ALI culture conditions ($n = 3$, mean ± SD).

strong enough to avoid a proper aerosolization. High ED and decent FPF values were achieved in all Co-SD powders. By decreasing the amount of the hygroscopic L-Car salt, the residual water content also decreased in all the systems. This was seen in the 80:20 systems which had a very low residual water content in comparison with the 50:50 system. Sim is a very hydrophobic drug, so it did not adsorb moisture while it was in contact with the environment. In contrast to Sim, L-Car did. These values were acceptable for dry powder inhalation aerosol formulations. The low residual water content in all the systems also played a role in their deposition. In DPI powders, residual water needs to be reduced since it is known to have a significant effect on DPI characteristics such as aerosolization of the particles, particle size distribution, crystallinity, and stability. Likewise, capillary forces can be extensively reduced by having low residual water content.[21,39] In general, better aerosolization was achieved with the 0.5% w/v systems. The MMAD values were smaller and therefore the FPF and RF values had an impact, showing higher numbers. This was in good agreement with the literature which says that SD more diluted solutions give smaller particles. The comparison between the two DPI devices showed that in general, this Co-SD systems aerosolized better with the NeoHaler device, a medium shear stress device.

By observing the 3-D surface response plots (Figure 16) using Design-Expert 8.0.7.1 software (StatEase Corporation, Minneapolis, MN), it was clearly observed that there was no significant statistical difference in the ED by changing the start feed solution concentration or by changing the DPI devices. Regarding the RF, there was a significant statistical difference by changing the start solution concentration, favoring the lower one. There was an observable statistical difference by changing the DPI devices, although not in all systems. Only the 80:20 molar ratio showed statistical difference in RF by changing the DPI device. The same trend was observed in FPF where there was a significant statistical difference by changing the start solution concentration. Also, only for the 80:20 system, the difference was significant using different devices. The last parameter analyzed was the MMAD which did not show a significant statistical difference by changing feed solution concentration or by using different DPI devices.

Acosta et al. (2021),[15] showed NGI results with excellent aerosol performance, with an ED exceeding 90% for all three DPI devices tested (i.e., HandiHaler, NeoHaler, and Aerolizer). The FPF, which indicates the percentage of particles small enough (<5 μm) to reach the deep lung, was particularly high for powders produced at lower pump rates and feed concentrations. In this cospray drying study, the NGI results were similarly favorable, as were and the ED and RF values. The smooth surface morphology of these Co-SD particles facilitated efficient aerosolization. The FPF values for Co-SD Sim and L-Car formulations were in the range of 6.86−12.13% depending on the molar ratio and DPI device. A major advantage is in dual-drug inhalation aerosol delivery, which targets simultaneously and colocalize at the deposition site, enhancing the therapeutic effect. This is well-established in the clinical treatment of other lung diseases including asthma and COPD. Sim offers anti-inflammatory and antioxidant properties and prevents vascular remodeling. L-Car supports mitochondrial function and reduces oxidative stress, providing a synergistic effect with Sim.

Moreover, these Co-SD formulations showed substantial improvement in aerosol dispersion and aerosol parameters compared to L-Car alone.[19] Greater FPF values of the Co-SD
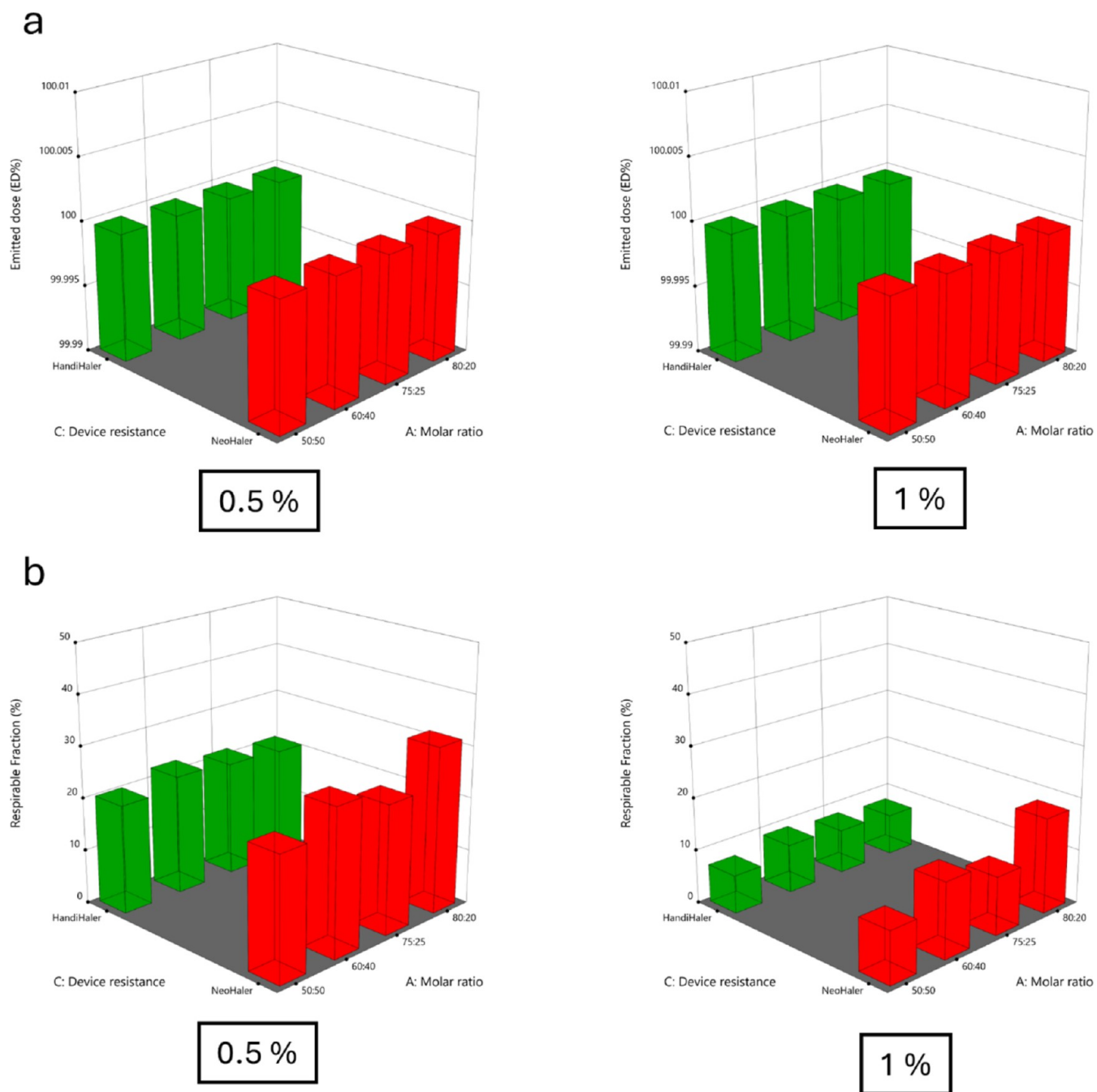
Figure 16. continued
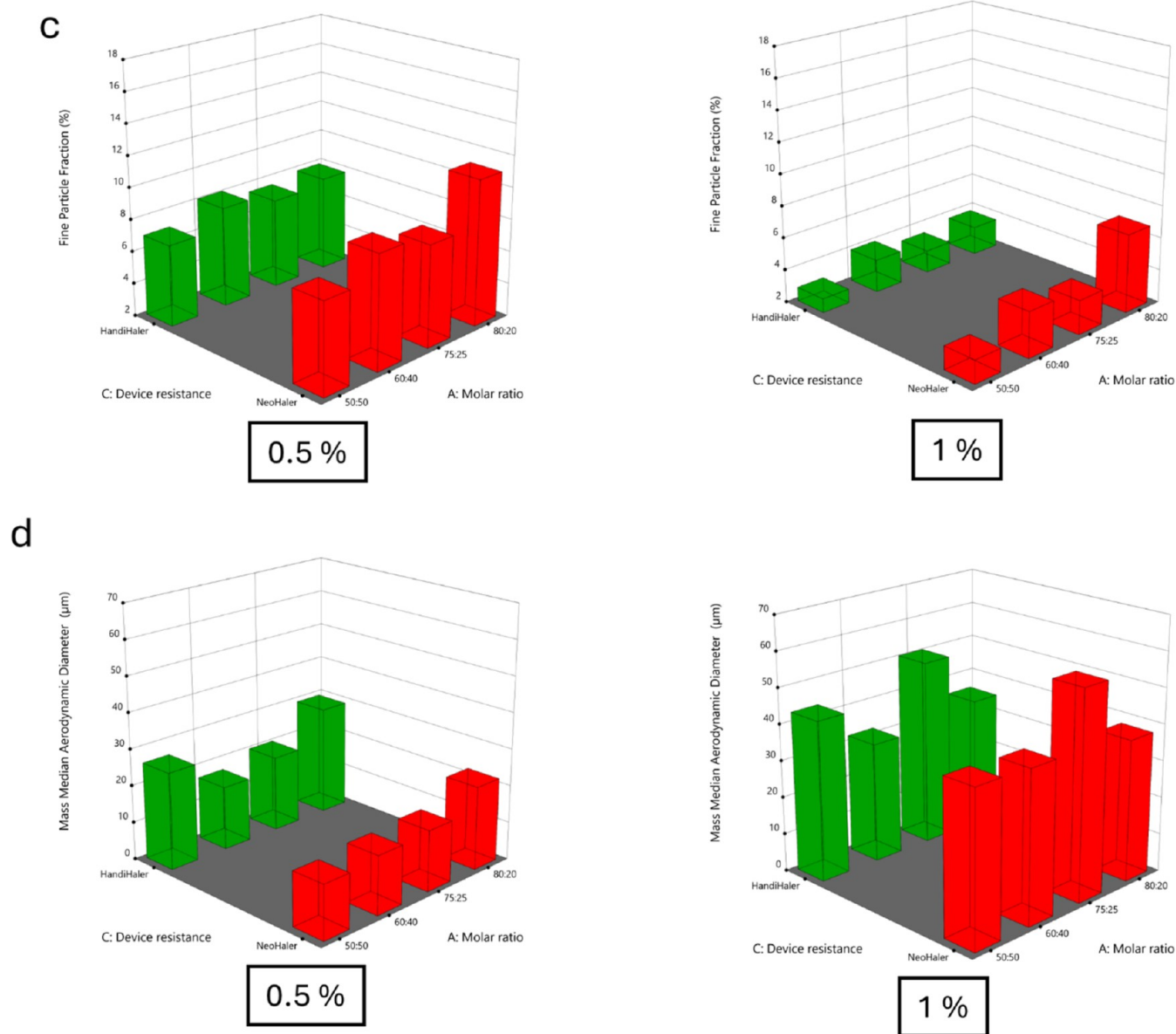
Figure 16. 3-D surface response plots showing the influence of the molar ratio and the different DPI devices on the in vitro aerosol dispersion performance of Co-SD Sim/L-Car HCl powder formulations for (a) % ED; (b) % RF; (c) % FPF; and (d) MMAD (μm).

DPIs compared to SD L-Car DPI powders was also achieved in this study.

Retention of crystallinity after SD was demonstrated in all Co-SD systems. XRPD diffraction pattern (Figure 5) showed sharp peaks in all powders which were attributable to the long-range molecular order due to the crystallinity of the drugs. The molar ratio and/or SD parameters had no apparent effect on the XRPD diffractograms. DSC thermograms (Figures 6 and 7) also confirmed the presence of crystalline composites. Fast DSC heating scans were conducted at 20 and 40 °C/min on all systems and no T_g was detected (data not shown). This confirmed that the powders were crystalline which agreed well with the XRPD diffractograms (Figure 5). Moreover, the DSC thermograms (Figures 6 and 7) suggested a molecular mixture formed between Sim and L-Car after SD. This is evident by the single-phase transition which corresponded to the melting of the mixture and suggested a homogeneous molecular mixture and the temperature of melting of the mixture was not close to the melting temperature of pure Sim nor pure L-Car.

HSM (Figure 8) enabled the visualization of the particles as a function of temperature and confirmed the phase transitions of the DPIs. It also demonstrated the thermostability of the particles at room and physiological temperatures. The temperature of melting of the mixtures agreed with the DSC thermograms (Figures 6 and 7). In the HSM images, birefringence was observable. This also confirmed the crystallinity of the powders which was in excellent agreement with the DSC thermograms and XRPD diffractograms.

ATR-FTIR molecular fingerprinting spectra (Figures 9 and 10) of the Co-SD systems had peaks matching with both Sim and L-Car and other peaks that might be a reference of the bonds that were forming after SD, which were confirming the molecular mixture. Characteristic bands of both molecules were seen in the spectra, such as the band corresponding to the OH group and the bands corresponding to the stretching vibration of ester and lactone carbonyl functional group of Sim; and the bands corresponding to L-Car such as the ones corresponding to the CN group. The in vitro 2D cell and 3D

lung tissue culture viability on various human lung cell and tissue types and TEER demonstrated that these formulations were safe at different concentrations and on different human pulmonary cell types under the conditions studied.

CONCLUSIONS

Dry powder aerosol powders of Sim with L-Car were rationally designed and successfully developed by organic solution advanced cospray drying from two different dilute solute feed concentrations. This comprehensive and systematic study is the first to report on the design, development, and characterization of innovative Co-SD dual-drug combination of a Nrf2 activator ROCK inhibitor (Sim)/ L-Car in various ratios for targeted pulmonary inhalation delivery in PH. The two components were spray dried at various molar ratios using different starting feed solution concentrations and process parameters. In addition to comprehensive physicochemical characterization, in vitro aerosol dispersion performance as DPIs using two FDA-approved DPI devices with different shear stress properties, in vitro viability as a function of dose on 2D human pulmonary cellular monolayers and on 3D small airway epithelia human primary cultures at the ALI, and in vitro TEER at the ALI were conducted. Solid-state physicochemical characterization confirmed homogeneous molecular mixtures and the crystalline nature of the Co-SD formulations. In vitro aerosolization dispersion performance demonstrated that all Co-SD dual combination molecular mixtures aerosolized successfully with both human FDA-approved DPI devices, had ~100% ED, and good FPF values. The in vitro viability and TEER assays demonstrated that all formulations were safe to human pulmonary 2D and 3D cultures as a function of dose.

AUTHOR INFORMATION

Corresponding Author

Heidi M. Mansour — *The University of Arizona College of Pharmacy, Skaggs Pharmaceutical Sciences Center, Tucson, Arizona 85721, United States; Florida International University, Center for Translational Science, Port St. Lucie, Florida 34987, United States; Florida International University, Robert Stempel College of Public Health and Social Work, Department of Environmental Health Sciences, Miami, Florida 34987, United States; The University of Arizona College of Medicine, Department of Medicine, Division of Translational and Regenerative Medicine, Tucson, Arizona 85724, United States; Florida International University, Herbert Wertheim College of Medicine, Department of Cellular & Molecular Medicine, Miami, Florida 33199, United States; Florida International University, College of Engineering and Computing, Department of Biomedical Engineering, Miami, Florida 33174, United States;* ⊙ orcid.org/0000-0003-3993-9210; Phone: (772) 345-4731; Email: hmansour@fiu.edu

Authors

Maria F. Acosta — *The University of Arizona College of Pharmacy, Skaggs Pharmaceutical Sciences Center, Tucson, Arizona 85721, United States*

David Encinas-Basurto — *The University of Arizona College of Pharmacy, Skaggs Pharmaceutical Sciences Center, Tucson, Arizona 85721, United States; Universidad de Sonora, Department of Physics, Nanotechnology Program, Hermosillo, Sonora 83000, México*

Michael D. Abrahamson — *The University of Arizona College of Pharmacy, Skaggs Pharmaceutical Sciences Center, Tucson, Arizona 85721, United States*

Basanth Babu Eedara — *The University of Arizona College of Pharmacy, Skaggs Pharmaceutical Sciences Center, Tucson, Arizona 85721, United States; Florida International University, Center for Translational Science, Port St. Lucie, Florida 34987, United States; Florida International University, Robert Stempel College of Public Health and Social Work, Department of Environmental Health Sciences, Miami, Florida 34987, United States*

Don Hayes, Jr. — *The Ohio State University College of Medicine, the Davis Heart and Lung Research Institute, Columbus, Ohio 43271, United States; Cincinnati Children's Medical Center, Cincinnati, Ohio 45229, United States*

Jeffrey R. Fineman — *University of California San Francisco School of Medicine, Department of Pediatrics, San Francisco, California 94107, United States*

Stephen M. Black — *Florida International University, Center for Translational Science, Port St. Lucie, Florida 34987, United States; Florida International University, Robert Stempel College of Public Health and Social Work, Department of Environmental Health Sciences, Miami, Florida 34987, United States; The University of Arizona College of Medicine, Department of Medicine, Division of Translational and Regenerative Medicine, Tucson, Arizona 85724, United States; Florida International University, Herbert Wertheim College of Medicine, Department of Cellular & Molecular Medicine, Miami, Florida 33199, United States*

Complete contact information is available at:
https://pubs.acs.org/10.1021/acsbiomedchemau.4c00063

Author Contributions

CRediT: **Maria F Acosta** data curation, formal analysis, funding acquisition, investigation, methodology, resources, software, validation, visualization, writing - original draft, writing - review & editing; **David Encinas-Basurto** data curation, formal analysis, funding acquisition, investigation, methodology, resources, software, validation, visualization, writing - original draft, writing - review & editing; **Michael D. Abrahamson** data curation, investigation, methodology, software, writing - original draft, writing - review & editing; **Basanth Babu Eedara** data curation, formal analysis, investigation, software, visualization, writing - review & editing; **Don Hayes, Jr** conceptualization, formal analysis, investigation, writing - review & editing; **Jeffrey R Fineman** conceptualization, funding acquisition, investigation, methodology, resources, visualization, writing - review & editing; **Stephen M Black** conceptualization, funding acquisition, investigation, project administration, resources, supervision, visualization, writing - original draft, writing - review & editing; **Heidi M. Mansour** conceptualization, data curation, formal analysis, funding acquisition, investigation, methodology, project administration, resources, software, supervision, validation, visualization, writing - original draft, writing - review & editing.

Notes

The authors declare no competing financial interest.

ACKNOWLEDGMENTS

■ REFERENCES

(1) Labiris, N. R.; Dolovich, M. B. Pulmonary drug delivery. Part I: Physiological factors affecting therapeutic effectiveness of aerosolized medications. *Br. J. Clin. Pharmacol.* **2003**, *56* (6), 588−599.

(2) Mansour, H. M.; Myrdal, P. B.; Younis, U. S.; Muralidharan, P.; Hillery, A. M.; Hayes, D. J. Chapter 11: Pulmonary drug delivery. In *Drug Delivery: Fundamentals & Applications*; Hillery, A. M., Swarbrick, J., Park, K., Eds.; CRC Press/Taylor & Francis, 2016; pp 249−277.

(3) Hickey, A. J.; Mansour, H. M. Chapter 5: Delivery of drugs by the pulmonary route. In *Modern Pharmaceutics*, 5th ed.; Florence, A. T., Siepmann, J., Eds.; Taylor & Francis, 2009; pp 191−219.

(4) Eedara, B. B.; Alabsi, W.; Encinas-Basurto, D.; Polt, R.; Hayes, D. J.; Black, S. M.; Mansour, H. M. Pulmonary drug delivery. In *Organelle and Molecular Targeting*; Milane, L., Amiji, M., Eds.; CRC Press/Taylor & Francis, 2021; pp 227−278.

(5) Cheng, Y. S. Mechanisms of pharmaceutical aerosol deposition in the respiratory tract. *AAPS PharmSciTech* **2014**, *15* (3), 630−640.

(6) Muralidharan, P.; Hayes, D., Jr.; Mansour, H. M. Dry powder inhalers in COPD, lung inflammation and pulmonary infections. *Expert Opin. Drug Delivery* **2015**, *12* (6), 947−962.

(7) Wu, X.; Li, X.; Mansour, H. M. Surface analytical techniques in solid-state particle characterization for predicting performance in dry powder inhalers. *KONA Powder Part. J.* **2010**, *28* (0), 3−19.

(8) Eedara, B. B.; Alabsi, W.; Encinas-Basurto, D.; Polt, R.; Mansour, H. M. Spray-dried inhalable powder formulations of therapeutic proteins and peptides. *AAPS PharmSciTech* **2021**, *22* (5), 185.

(9) Meenach, S. A.; Anderson, K. W.; Hilt, J. Z.; McGarry, R. C.; Mansour, H. M. High-performing dry powder inhalers of paclitaxel DPPC/DPPG lung surfactant-mimic multifunctional particles in lung cancer: physicochemical characterization, in vitro aerosol dispersion, and cellular studies. *AAPS PharmSciTech* **2014**, *15* (6), 1574−1587.

(10) Oishi, P.; Fineman, J. R. Pulmonary hypertension. *Pediatr. Crit. Care Med.* **2016**, *17* (8), S140−S145.

(11) de Jesus Perez, V. A. Molecular pathogenesis and current pathology of pulmonary hypertension. *Heart Fail. Rev.* **2016**, *21*, 239−257.

(12) Gan, C. T.; Noordegraaf, A. V.; Marques, K. M. J.; Bronzwaer, J. G. F.; Postmus, P. E.; Boonstra, A. A review of pulmonary arterial hypertension: Part 1. Novel insights and classification. *Neth. Heart J.* **2004**, *12* (6), 287−294.

(13) Runo, J. R.; Loyd, J. E. Primary pulmonary hypertension. *Lancet* **2003**, *361* (9368), 1533−1544.

(14) Acosta, M. F.; Hayes, D. J.; Fineman, J. R.; Yuan, J. X.-J.; Black, S. M.; Mansour, H. M. Chapter 19: Therapeutics in pulmonary hypertension. In *Inhalation Aerosols: Physical and Biological Basis for Therapy*, 3rd ed.; Hickey, A. J., Mansour, H. M., Eds.; CRC Press/Taylor & Francis, 2019; pp 313−322.

(15) Acosta, M. F.; Muralidharan, P.; Grijalva, C. L.; Abrahamson, M. D.; Hayes, D., Jr.; Fineman, J. R.; Black, S. M.; Mansour, H. M. Advanced therapeutic inhalation aerosols of a Nrf2 activator and

(16) Zivkovic, S.; Maric, G.; Cvetinovic, N.; Lepojevic-Stefanovic, D.; Bozic Cvijan, B. Anti-inflammatory effects of lipid-lowering drugs and supplements—a narrative review. *Nutrients* **2023**, *15* (6), 1517.

(17) Keshavarz, A.; Kadry, H.; Alobaida, A.; Ahsan, F. Newer approaches and novel drugs for inhalational therapy for pulmonary arterial hypertension. *Expert Opin. Drug Delivery* **2020**, *17* (4), 439−461.

(18) Sharma, S.; Aramburo, A.; Rafikov, R.; Sun, X.; Kumar, S.; Oishi, P. E.; Datar, S. A.; Raff, G.; Xoinis, K.; Kalkan, G.; et al. L-Carnitine preserves endothelial function in a lamb model of increased pulmonary blood flow. *Pediatr. Res.* **2013**, *74* (1), 39−47.

(19) Acosta, M. F.; Muralidhran, P.; Abrahamson, M. D.; Grijalva, C. L.; Carver, M.; Tang, H.; Klinger, C.; Fineman, J. R.; Black, S. M.; Mansour, H. M. Comparison of L-carnitine and L-carnitine HCL salt for targeted lung treatment of pulmonary hypertension (PH) as inhalation aerosols: design, comprehensive characterization, in vitro 2D/3D cell cultures, and in vivo MCT-Rat model of PH. *Pulm. Pharmacol. Ther.* **2020**, *65*, 101998.

(20) Duan, J.; Vogt, F. G.; Li, X.; Hayes, D., Jr.; Mansour, H. M. Design, characterization, and aerosolization of organic solution advanced spray-dried moxifloxacin and ofloxacin dipalmitoylphosphatidylcholine (DPPC) microparticulate/nanoparticulate powders for pulmonary inhalation aerosol delivery. *Int. J. Nanomed.* **2013**, *8*, 3489−3505.

(21) Li, X.; Vogt, F. G.; Hayes, D., Jr.; Mansour, H. M. Design, characterization, and aerosol dispersion performance modeling of advanced co-spray dried antibiotics with mannitol as respirable microparticles/nanoparticles for targeted pulmonary delivery as dry powder inhalers. *J. Pharm. Sci.* **2014**, *103* (9), 2937−2949.

(22) Meenach, S. A.; Anderson, K. W.; Zach Hilt, J.; McGarry, R. C.; Mansour, H. M. Characterization and aerosol dispersion performance of advanced spray-dried chemotherapeutic PEGylated phospholipid particles for dry powder inhalation delivery in lung cancer. *Eur. J. Pharm. Sci.* **2013**, *49* (4), 699−711.

(23) Willis, L.; Hayes, D., Jr.; Mansour, H. M. Therapeutic liposomal dry powder inhalation aerosols for targeted lung delivery. *Lung* **2012**, *190* (3), 251−262.

(24) Wu, X.; Hayes, D., Jr.; Zwischenberger, J. B.; Kuhn, R. J.; Mansour, H. M. Design and physicochemical characterization of advanced spray-dried tacrolimus multifunctional particles for inhalation. *Drug Des. Dev. Ther.* **2013**, *7*, 59−72.

(25) Muralidharan, P.; Mallory, E. K.; Malapit, M.; Phan, H.; Ledford, J. G.; Hayes, D., Jr.; Mansour, H. M. Advanced design and development of nanoparticle/microparticle dual-drug combination lactose carrier-free dry powder inhalation aerosols. *RSC Adv.* **2020**, *10* (68), 41846−41856.

(26) Muralidharan, P.; Hayes, D.; Black, S. M.; Mansour, H. M. Microparticulate/nanoparticulate powders of a novel Nrf2 activator and an aerosol performance enhancer for pulmonary delivery targeting the lung Nrf2/Keap-1 pathway. *Mol. Syst. Des. Eng.* **2016**, *1* (1), 48−65.

(27) The United States Pharmacopoeia and The National Formulary. ⟨601⟩ Aerosols, nasal sprays, metered-dose inhalers, and dry powder inhalers monograph. *USP 29-NF 24: The Official Compendia of Standards 29/24*; The United States Pharmacopeial Convention, 2006; pp 2617−2636.

(28) Krüger, P.; Ehrlein, B.; Zier, M.; Greguletz, R. Inspiratory flow resistance of marketed dry powder inhalers (DPI). *Eur. Respir. J.* **2014**, *44* (Suppl 58), 4635.

(29) Mueller, S.; Haeberlin, B.; Edge, S. Comparison of performance characteristics for Foradil Aerolizer and Foradil Concept1 (a new single dose dry powder inhaler) at different test flow rates. *Respir. Drug Delivery* **2008**, *3*, 675−678.

(30) Acosta, M. F.; Muralidharan, P.; Meenach, S. A.; Hayes, D.; S, M. B.; Mansour, H. M. In vitro pulmonary cell culture in pharmaceutical

inhalation aerosol delivery: 2-D, 3-D, and in situ bioimpactor models. *Curr. Pharm. Des.* **2016**, *22* (17), 2522−2531.

(31) Acosta, M. F.; Abrahamson, M. D.; Encinas-Basurto, D.; Fineman, J. R.; Black, S. M.; Mansour, H. M. Inhalable nanoparticles/microparticles of an AMPK and Nrf2 activator for targeted pulmonary drug delivery as dry powder inhalers. *AAPS J.* **2021**, *23* (1), 2.

(32) Salomon, J. J.; Muchitsch, V. E.; Gausterer, J. C.; Schwagerus, E.; Huwer, H.; Daum, N.; Lehr, C.-M.; Ehrhardt, C. The cell line NCl-H441 is a useful in vitro model for transport studies of human distal lung epithelial barrier. *Mol. Pharm.* **2014**, *11* (3), 995−1006.

(33) Ren, H.; Birch, N. P.; Suresh, V. An optimised human cell culture model for alveolar epithelial transport. *PLoS One* **2016**, *11* (10), No. e0165225.

(34) Epithelix SmallAir: a unique 3D human small airway epithelia reconstituted in vitro. http://www.epithelix.com/products/smallair (accessed January, 2019).

(35) Wong, M. J.; Kantores, C.; Ivanovska, J.; Jain, A.; Jankov, R. P. Simvastatin prevents and reverses chronic pulmonary hypertension in newborn rats via pleiotropic inhibition of RhoA signaling. *Am. J. Physiol. Lung Cell Mol. Physiol.* **2016**, *311* (5), L985−L999.

(36) Chew, N. Y.; Chan, H.-K. Use of solid corrugated particles to enhance powder aerosol performance. *Pharm. Res.* **2001**, *18* (11), 1570−1577.

(37) Nair, V. V.; Smyth, H. D. Inhalable excipient-free dry powder of tigecycline for the treatment of pulmonary infections. *Mol. Pharm.* **2023**, *20* (9), 4640−4653.

(38) Quarta, E.; Chierici, V.; Flammini, L.; Tognolini, M.; Barocelli, E.; Cantoni, A. M.; Dujovny, G.; Ecenarro Probst, S.; Sonvico, F.; Colombo, G.; et al. Excipient-free pulmonary insulin dry powder: pharmacokinetic and pharmacodynamics profiles in rats. *J. Controlled Release* **2020**, *323*, 412−420.

(39) Pilcer, G.; Amighi, K. Formulation strategy and use of excipients in pulmonary drug delivery. *Int. J. Pharm.* **2010**, *392* (1−2), 1−19.